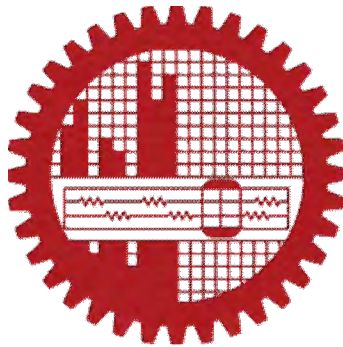# Impact of Intra-Channel Cross-Phase Modulation on High Speed Optical Fiber Communication System

By

Nitu Syed

MASTER OF SCIENCE IN ELECTRICAL AND ELECTRONIC ENGINEERING

Department of Electrical and Electronic Engineering

BANGLADESH UNIVERSITY OF ENGINEERING AND TECHNOLOGY

June 2012

The thesis titled **"Impact of Intra-Channel Cross-Phase Modulation on High Speed Optical Fiber Communication System"** submitted by Nitu Syed, Student No: 1009062021, Session: October,2009, has been accepted as satisfactory in partial fulfillment of the requirement for the degree of MASTER OF SCIENCE IN ELECTRICAL AND ELECTRONIC ENGINEERING on June 16, 2012.

BOARD OF EXAMINERS

1._____

Dr. Mohammad Faisal
Assistant Professor
Department of Electrical and Electronic Engineering,   Chairman
Bangladesh University of Engineering and Technology (BUET),   (Supervisor)
Dhaka – 1000, Bangladesh.

2._____

Dr. Pran Kanai Saha
Professor and Head   Member
Department of Electrical and Electronic Engineering,   (Ex-officio)
Bangladesh University of Engineering and Technology (BUET)
Dhaka – 1000, Bangladesh

3._____

Dr. Md. Saiful Islam
Professor, IICT, BUET   Member
Dhaka – 1000, Bangladesh.

4._____

Dr. Md. Shah Alam
Professor
Department of Electrical and Electronic Engineering, BUET   Member
Dhaka – 1000, Bangladesh.

5._____

Dr. Khawza I. Ahmed
Associate Professor
Dept of EEE, United International University,   Member
UIU Bhaban, House#80, Satmosjid Road,   (External)
Dhanmondi, Dhaka -1209

CANDIDATE'S DECLARATION

It is hereby declared that this thesis or any part of it has not been submitted elsewhere for the award of any degree or diploma and that all sources are acknowledged.

Signature of the Candidate

_____

Nitu Syed

Dedication

To my parents and husband.

Acknowledgement

First of all, I would like to thank Allah for giving me the ability to complete this thesis work.

I would like to express my sincere gratitude to my supervisor, Dr.Mohammad Faisal. This thesis would not have been completed without his support and guidance. I would like to express my great thanks and gratefulness for his instructions, continuous encouragement, valuable discussions, and careful review during the period of this research. His keen sight and a wealth of farsighted advice and supervision have always provided me the precise guiding frameworks of this research. I have learned many valuable lessons and concepts of Optical fiber Communication from him through my study, which I have utilized to develop my abilities to work innovatively and to boost my knowledge. His constant encouragement gave me the confidence to carry out my work.

I would like to thank all my teachers. They gave the knowledge and directions that have helped me throughout my life. I express my gratitude to my teachers from Bangladesh University of Engineering and Technology. The knowledge I learned from the classes in my M.Sc. levels were essential for this thesis.

Special thanks go to Fahim and Oishik, my two junior friends from the Department of Electrical and Electronic Engineering (EEE), BUET for their support in conducting my research. I also want to thank my friends for providing my support and encouragement. Their suggestions helped me in countless ways.

Last but not the least, I would like to thank by parents and my family. Their unconditional support made it possible for me to finish this thesis.

ABSTRACT

In this thesis, analytical estimation of phase fluctuations due to intra-channel cross-phase modulation (IXPM) on return-to-zero (RZ) pulse has been studied in details for both uncompensated single line transmission and periodically dispersion managed (DM) system. We have investigated optical pulse propagation operating at a speed of 40 Gb/s for both systems. The basic theories for the analyses employed in this thesis for optical pulse transmission is presented after making a brief discussion on fiber nonlinearities. First fundamental equations of optical pulse propagation in a fiber have been studied assuming a suitable solution for the Nonlinear Schrödinger (NLS) equation. Here we use variational method to examine the IXPM induced phase fluctuation analytically. Various dynamical equations have been derived with IXPM as a source of perturbation. We have obtained several ordinary differential equations for various pulse parameters. These pulse parameters are amplitude (A), reciprocal of pulse width (p), linear chirp (C), central frequency (κ), central time position (T) and the phase of the pulse (θ). These ordinary differential equations have been solved by Runge-Kutta method to find out the phase fluctuations due to intra-channel cross-phase modulation.

The effects of IXPM induced phase fluctuation with the variation of different parameters have been explored for both uncompensated single line transmission and DM system. The amount of phase shift is investigated by changing different parameters such as transmission distance, input power, duty cycle, bit-rate and dispersion map strength. Different transmission models will be explored to check an optimum model. Finally, split-step Fourier method (SSFM) is used in some cases to achieve the full numerical simulation and to validate the accuracy of proposed analytical models.

CONTENTS

LIST OF FIGURES

LIST OF ABBREVIATIONS

BER	:	Bit Error Rate
CD	:	Chromatic Dispersion
DCF	:	Dispersion Compensating Fiber
DM	:	Dispersion Managed
DPSK	:	Differential Phase Shift Keying
DQPSK	:	Differential Quadrature Phase Shift Keying
EDFA	:	Erbium-doped Fiber Amplifier
FWM	:	Four Wave Mixing
GVD	:	Group Velocity Dispersion
IFWM	:	Intra-Channel Four-Wave Mixing
IXPM	:	Intra-Channel Cross-Phase Modulation
NLPN	:	Nonlinear Phase Noise
NLSE	:	Nonlinear Schroedinger Equation
NZDSF	:	Non-zero Dispersion–Shifted Fiber
OOK	:	On-Off Keying
QPSK	:	Quadrature Phase Shift Keying
SBS	:	Stimulated Brillouin Scattering
SNR	:	Signal to Noise Ratio
SPM	:	Self Phase Modulation
SRS	:	Stimulated Raman Scattering
SSFM	:	Split-Step Fourier Method
SSMF	:	Standard Single Mode Fiber
XPM	:	Cross Phase Modulation

LIST OF SYMBOLS

n	:	Refractive index
n_2	:	Nonlinear refractive index of fiber
E	:	Electric field
$\Delta\omega$	:	Spectral width of pulse
β	:	Propagation constant
c	:	Speed of light in vacuum
β_1	:	Inverse group velocity
β_2	:	Second order dispersion coefficient
z_{eff}	:	Effective transmission distance
α	:	Attenuation coefficient
λ	:	Wavelength of light
D	:	Dispersion parameter
λ_D	:	Zero dispersion wavelength.
L_D	:	Dispersion length
ϕ_{NL}	:	Nonlinear phase shift
ϕ_L	:	Linear phase shift
γ	:	Kerr nonlinear coefficient
A_{eff}	:	Effective core area
$b(Z)$	:	Normalized dispersion profile
$S(Z)$	:	Normalized fiber nonlinearity
$\Gamma(Z)$	:	Normalized loss
Z_a	:	Amplifier spacing
R	:	Perturbation
A	:	Amplitude of pulse
E_j	:	Pulse energy

p	:	Inverse of pulse width
C	:	Linear chirp
κ	:	Central frequency of pulse
T_0	:	Central time position of pulse
θ	:	Phase of the pulse
P	:	Power
d	:	Duty cycle
R_b	:	Bit rate
S	:	Dispersion map strength
τ_F	:	Minimum pulse width (FWHM).

CHAPTER 1

INTRODUCTION

1.1 Optical Fiber Communication

The advances in data communication and information technology allow tremendous amounts of data to be transferred through the networks. This is supported by high bandwidth optical fiber and also the emergence of fast computer processors, whose speed increases every day. As a result, all business activities which require high data bandwidth such as Video on Demand, video conferencing, digital photography and others can be conveniently realized. From one year to another, the required network capacity increases exponentially, which shows that Tbit/s capacity is not far from reality. On-off keying (OOK) based wavelength division multiplexing (WDM) transmission systems are the current technology for lightwave communications. Due to increased demand of global broadband date services and advanced Internet applications, networks based on fiber-optics are getting huge popularity and facing more and more pressure to cope up with demand. The next generation lightwave transmission systems should provide high capacity and at the same time, at a lower cost. This shifts the research trend from OOK-based system to the advanced modulation formats such as differential phase shift keying (DPSK), differential phase amplitude shift keying (DPASK), amplitude phase shift keying (APSK), and multilevel PSK/DPSK etc. to enhance the per-fiber transmission capacity [1]. Enhancing the spectral efficiency of a WDM network is considered as an economical way to expand the system capacity. For these reasons, in recent years, the differential phase modulation schemes, particularly DPSK and differential quadrature phase shift keying (DQPSK),draw huge research attention and are becoming the promising transmission formats for next generation spectrally efficient high speed long-haul optical transmission networks [2-4].

Phase modulated data formats like PSK and differential PSK have compact spectrum with constant envelope which yield some advantages over other data formats. They are, particularly differential PSK is robust to fiber dispersion and nonlinearity and have low intrachannel effects at high bit rate ($\geq$ 40 Gb/s) [5]. Recently, with advantage of fiber amplifiers like EDFA, direct detection for differential phase modulation schemes are

becoming popular because of simpler receiver structure with the merits of phase modulation and low-cost implementation. However, we can strongly predict that the phase modulation formats with high spectral efficiency are attractive alternatives to upgrade the capacity of currently deployed fiber-optic transmission systems.

1.2 Background

In this section, some features and limitations of phase modulated formats are briefly described referring to some recent researches. Phase modulated transmission systems are becoming promising data transmission scheme for future lightwave communications, which was rediscovered in 1999 by Atia et al. [6]. In PSK format, message lies in phase, whereas in DPSK transmissions, information is coded into the phase difference rather than phase. It is also experimentally proved that DPSK provides better performance at 40 Gb/s [7]. Among these, quadrature phase shift keying (QPSK) is becoming the most promising because of its superior transmission characteristics. These schemes require coherent detection and even after advancement in EDFA, it can provide better receiver sensitivity than OOK. In 2005, Gagnon et al. [8] has reported a QPSK transmission with coherent detection and digital signal processing (DSP) which can provide higher SNR (i.e., higher bit error rate (BER) performance) over the conventional differential detection without phase locking of the local oscillator to the carrier phase. However, we can strongly predict that the phase modulation formats with high spectral efficiency are attractive alternatives to upgrade the capacity of currently deployed fiber-optic transmission systems.

A lot of researches and development efforts have been done on advanced optical modulation schemes, both theoretically and experimentally, to address different aspects of those formats, and consequently to implement phase-modulated signals on currently deployed Metro networks. Fiber nonlinearity could be the essential limiting concern for long-haul fiber-optic transmission. All these nonlinear effects are locally rather small, but they become important by accumulation over long fiber lengths. They generally degrade the performance, transmission quality through signal losses, intra or interchannel crosstalks, pulse broadening or induced jitters. The physical impairments of optical fiber transmission can be categorized into two main parts irrespective of modulation/detection schemes: linear and nonlinear. Linear barriers include fiber loss and dispersion, and nonlinear part comprises interchannel and intrachannel

impairments. Interchannel impairments are self phase modulation (SPM), cross phase modulation (XPM), and four wave mixing (FWM). For phase modulation formats, phase noise induced by SPM is realized to be the major performance limiting factor for long distance lightwave communication systems [9].The phase noise impedes the phase modulated lightwave system by corrupting the phase of the signal which conveys the information. Phase fluctuation induced by XPM is also a great concern for WDM systems with phase modulation formats. The nonlinear effect XPM is caused by the modulation of refractive index by the total optical power in the fiber.XPM would result in the modulation of the optical phase and the intensity of various signals would be affected. Recently research on XPM has increased dramatically [10-12].

On the other hand, intra-channel cross-phase modulation (IXPM) and intra-channel four-wave mixing (IFWM) are the dominating intra-channel nonlinearities. In transmission systems operating at 40 Gb/s and above, intra-channel nonlinear effects IXPM and IFWM are more dominant rather than inter-channel interactions. Chromatic dispersion (CD) lets neighboring pulses overlap. As a result two effects IXPM and IFWM are introduced. These two effects were demonstrated for the first time by Essiambre et. al. [13] where they were suggested as the limiting factors in high speed OOK Time Division Multiplexed (TDM) system. Nonlinear phase noise in single channel DPSK systems has been also analyzed by Zhang et al. [14] taking into account the intrachannel effect in a highly dispersive system. IXPM is an inter-pulses effect. It is a phase perturbation that occurs to a specified pulse, resulting from the phase of neighboring pulses, in the same WDM channel. This factor is known as a major contributor of Nonlinear Phase Noise (NLPN) [15].

Overlapping between adjacent pulses also introduces ghost pulses, which is known as IFWM [16]. IFWM ghost pulses interfere with neighboring pulses, because the level of zero bits to increase and the amplitude of one bit to fluctuate. It is found that the IFWM effect in DPSK systems is smaller and less dependent on the bit pattern [17]. In comparison to the combined effect of IXPM and ISPM induced NLPN, IFWM effect is considered insignificant [18]. But IXPM distortion directly contaminates the pulse phase. So among these nonlinearities IXPM is our concern as it hampers the phase-modulated signal formats severely [17,19]. IXPM is one of the major causes of performance degradation in optical transmission systems [20]. If phase of a particular

pulse changes, the information of PSK system may also change. So IXPM is a critical factor, limiting the quality of signal transmission. To preserve the transmitted information, the maximum amount of phase shift should be lower than the prescribed value. However, the analyses of phase fluctuations due to IXPM in phase modulated signal and their impact on fiber-optic transmission system has yet to be address completely. Recently some research on IXPM have been conducting [21] but the basic study with overall performance analyses due to IXPM distortion are still under research. Getting motivations from these facts, we shall examine the phase fluctuations due to IXPM and evaluate the impact on transmission system in our thesis.

1.3 Objectives of the Thesis

The thesis concentrates on the impact of intra-channel cross-phase modulation on high speed optical fiber transmission system. The work consists of derivation of analytical expressions and numerical simulations.

The objectives of this thesis are:

i. To develop the analytical model for phase fluctuations due to IXPM using variational analysis for single channel DM system. Different dynamical equations for pulse parameters are obtained presuming IXPM as perturbation. These equations are solved by Runge-Kutta method.

ii. To investigate phase shift influenced by IXPM by changing various parameters such as: transmission distance, duty cycle, bit rate, bit period, dispersion map strength and input power.

iii. To explore the phase fluctuations in uncompensated single fiber transmission for two systems. One system consists of standard single mode fiber (SSMF) only. In another system Non-zero dispersion–shifted fiber (NZDSF) is used for 50km propagation.

iv. To evaluate the phase shift in two models of dispersion managed (DM) transmission systems for 1000km propagation. One model consists of standard single mode fiber (SSMF) and dispersion compensating fiber (DCF). In another model Non-zero dispersion–shifted fiber (NZDSF) is followed by DCF.

v. The analytical results are verified by numerical simulation. The numerical simulations are performed using split-step Fourier method (SSFM).

The outcome of this thesis is the development of analytical model for phase fluctuations and the exploration of the parameters that could affect phase shift due to IXPM. Finally the optimum model will be investigated for designing ultra-high speed phase modulated transmission systems so that IXPM-induced phase fluctuations remain low.

1.4 Organization of the Thesis

The thesis consists of five chapters.

Chapter 1 contains introductory discussion on optical fiber communications emphasizing on basic modulation formats. The objectives and outlining of the thesis are presented here.

In chapter 2, we have focused on the impact of different impairments for ultra-high speed long-haul optical fiber transmission systems.

In Chapter 3, the basic theories for the analyses employed in this thesis for DM transmission will be presented. Fundamental equations of optical pulse propagation in a fiber have been studied. Analytical calculation of phase fluctuations due to IXPM on RZ pulse in details will be explained. Varational method will be described and coupled ordinary differential equations will be deduced assuming a suitable solution for the nonlinear Schrödinger (NLS) equation. For checking the results of analytic techniques, we have introduced a numerical technique known as Split Step Fourier Method (SSFM). The dispersion managed system is also focused in this chapter.

Chapter 4 provides the summary of the results for uncompensated single fiber transmission and dispersion managed (DM) transmission stating the significance of the parameters that could affect IXPM and to choose a DM model so that IXPM-induced phase fluctuations remain low. Finally the optimum model will be investigated for designing ultra-high speed phase modulated transmission systems.

Chapter 5 is the concluding chapter. It contains the summary of the work. The chapter also highlights scopes for future work. All references are placed at the end of this thesis.

CHAPTER 2

IMPAIRMENTS OF OPTICAL FIBER COMMUNICATION

2.1 Introduction

The response of any dielectric to light becomes nonlinear for intense electromagnetic fields, and optical fiber is no exception. The optical fiber medium can only be approximated as a linear medium when the launch power is sufficiently low. For the long-haul fiber optic transmission system and wideband wavelength division multiplexed (WDM) systems, the launch power must be increased to keep signal to noise ratio (SNR) high enough for the error-free detection at receiver. As the input power increases, the nonlinearity of fiber becomes significant and leading to severe performance degrading. Besides, transmission capacity can be further enhanced by increasing the channel bit rate. The channel bit rate is upgraded to 10 Gb/s from 2.5 Gb/s and it is predicting that the next generation light wave communications will be based on 40 Gb/s rate. However, this high bit rate systems will face many problems due to fiber dispersion and nonlinearity which are interrelated with transmitting power, number of channels, channel spacing ,bit rate and transmission length etc.

In this chapter, we will discuss the basic impairments in optical fiber communication in section 2.2. Sub-section 2.2.1 presents a brief discussion on linear impairments. Non linear impairments are presented in sub-section 2.2.2. The impacts of inter-channel and intra-channel nonlinearities are explained here. Finally, section 2.3 indicates our motivation for working with IXPM.

2.2 Impairments of Optical Fiber Communication

The physical impairments of optical fiber transmission can be categorized into two main parts irrespective of modulation/detection schemes: linear and nonlinear. Linear barriers include fiber loss and dispersion, and nonlinear part comprises interchannel and intrachannel impairments.
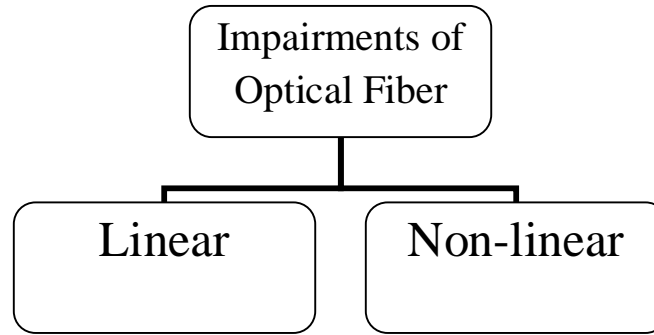
Fig.2.1: Impairments in optical fiber

Nonlinear effects in optical fibers are mainly due to two causes. One root cause lies in the fact that the refraction index of many materials, including glass, is a function of light intensity. The nonlinear response of refractive index under the influence of an applied field is called the Kerr effect and it was discovered in 1875 by John Kerr. The second root cause is the nonelastic scattering of photons in fibers, which results in stimulated Raman and stimulated Brillouin scattering phenomena. These are in addition to the dependence of the index of refraction on wavelength, which gives rise to dispersion effects. The refractive index of a fiber core can be written as

$$\tilde{n}(\omega, |E|^2) = n_0(\omega) + n_2 |E|^2 \tag{2.1}$$

or as $n = n_0 + n_2 \dfrac{P}{A_{eff}}$ (2.2)

Where n_0 is the linear part and n_2 is the nonlinear-index coefficient related to $\chi^{(3)}$ by the relation $n_2 = (3/8n) \, Re \, (\chi^{(3)})$. P is the power of the light wave inside the fiber and A_{eff} is the effective area of fiber core over which power is distributed. The intensity dependence of refractive index of silica leads to a large number of nonlinear effects, such as, SPM, XPM and FWM. The second mechanism for generating nonlinearities in fiber is the stimulated scattering phenomena. These mechanisms give rise to stimulated Brillouin scattering (SBS) and stimulated Raman scattering (SRS). Different fiber nonlinear effects are briefly narrated below:

2.2.1 Linear Impairment

In fiber optic communication systems, linear impairments are due to the fiber loss and chromatic dispersion (CD). Light traveling in an optical fiber loses power over distance.

The loss of power depends on the wavelength of the light and on the propagating material. For silica glass, the shorter wavelengths are attenuated the most. The lowest loss occurs at the 1550-nm wavelength, which is commonly used for long-distance transmissions. Transmission of light by fiber optics is not 100% efficient. There are several reasons for this including absorption by the core and cladding (caused by the presence of impurities) and the leaking of light from of the cladding. The loss of power in light in an optical fiber is measured in decibels (dB). Fiber optic cable specifications express cable loss as attenuation per 1-km length as dB/km. This value is multiplied by the total length of the optical fiber in kilometers to determine the fiber's total loss in dB.

Chromatic dispersion or group velocity dispersion (GVD) is primarily the cause of performance limitation in the long haul fiber optic communication systems. Dispersion is the spreading out of a light pulse in time as it propagates down the fiber. As a result short pulses broaden, which leads to significant intersymbol interference (lSI), and therefore, severely degrades the performance. Single mode fibers effectively eliminate inter-modal dispersion by limiting the number of modes to just one through a much smaller core diameter. However, the pulse broadening still occurs in SMFs due to intra-modal dispersion which is described as follows.When an electromagnetic wave interacts with the bound electrons of a dielectric, the medium response depends on the optical frequency (ω). This property manifests through the frequency dependence of the refractive index $n\ (\omega)$. Because the velocity of light is determined by $c/n(\omega)$, the different frequency components of the optical pulse would travel at different speeds. This phenomenon is called group velocity dispersion or chromatic dispersion to emphasize its frequency dependent nature. Assuming the spectral width of the pulse to be $\Delta\omega$, at the output of the optical fiber, the pulse broadening can be estimated as

$$\Delta T \approx L\frac{d^2\beta}{d\omega^2}\Delta\omega = L\beta_2\Delta\omega. \tag{2.3}$$

Where $\beta_2 = \dfrac{d^2\beta}{d\omega^2}$ is known as GVD Parameter and

L is the fiber length. It can be seen from eqn. (2.3), that the amount of pulse broadening is determined by the spectral width of pulse, $\Delta\omega$. The dispersion induced spectrum broadening would be very important even without nonlinearity for high data-rate transmission systems (> 2.5 Gb/s), and it could limit the maximum error-free transmission distance. The effects of dispersion can be described by expanding the

mode propagation constant, β at any frequency ω in terms of the propagation constant and its derivatives at some reference frequency ω_0 using Taylor Series,

$$\beta(\omega) = \beta_0 + \beta_1(\omega - \omega_0) + \frac{1}{2}\beta_2(\omega - \omega_0)^2 + ... \qquad (2.4)$$

Here $\beta_m(\omega) = \left[\dfrac{d^m\beta}{d\omega^m}\right]_{\omega=\omega_0} (m=0,1,2,......)$ $\qquad\qquad$ (2.5)

It is easy to get first-order and second-order derivatives from Eqns. (2.4) and (2.5)

$$\beta_1 = \frac{1}{c}\left[n + \omega\frac{dn}{d\omega}\right] = \frac{1}{v_g} \qquad (2.6)$$

and

$$\beta_2 = \frac{1}{c}\left[2\frac{dn}{d\omega} + \omega\frac{d^2n}{d\omega^2}\right] \approx \frac{\lambda^3}{2\pi c^2}\frac{d^2n}{d\lambda^2}, \qquad (2.7)$$

where c is the speed of light vacuum and λ is the wavelength. β_1 is the inverse group velocity, and β_2 is the second order dispersion coefficient. If the signal bandwidth is much smaller than the carrier frequency ω_0, we can truncate the Taylor series after the second term on the right hand side. As the spectral width of the signal transmitted over the fiber increases, it may be necessary to include the higher order dispersion coefficients such as β_3 and β_4. The wavelength where $\beta_2 = 0$ is called zero dispersion wavelength λ_D. Dispersion parameter, D, is another parameter related to the difference in arrival time of pulse spectrum. The relationship between D, β_1 and β_2 can be found as following

$$D = \frac{d\beta_1}{d\lambda} = -\frac{2\pi c}{\lambda^2}\beta_2 \approx -\frac{\lambda}{c}\frac{d^2n}{d\lambda^2} \qquad (2.8)$$

From Eq. (2.8) it can be understood that D has the opposite sign with β_2. If $\lambda < \lambda_D$, $\beta_2 < 0$ (or $D > 0$), It is said that optical signal exhibit anomolous dispersion. In the anomolous dispersion regime high-frequency components of optical signal travel faster than low-frequency components. On the contrary, When $\lambda > \lambda_D$, $\beta_2 > 0$ (or $D < 0$), it is said to exhibit normal dispersion. In the normal dispersion regime high frequency

components of optical signal travel slower than low-frequency components. The normal dispersion regime is of considerable interest for the study of nonlinear effects, because it is in this regime that optical fibers support solitons through a balance between the dispersive and nonlinear effects. The impact of the group velocity dispersion can be conventionally described using the dispersion length which is defined as [22]

$$L_D = \frac{T_0^2}{\beta_2} \qquad (2.9)$$

where T_0 is the temporal pulse width. This length provides a scale over which the dispersive effect becomes significant for pulse evolution along a fiber. Dispersion and specially GVD play an important role in signal transmission over fibers. The interaction between dispersion and nonlinearity is an important issue in light wave system design.
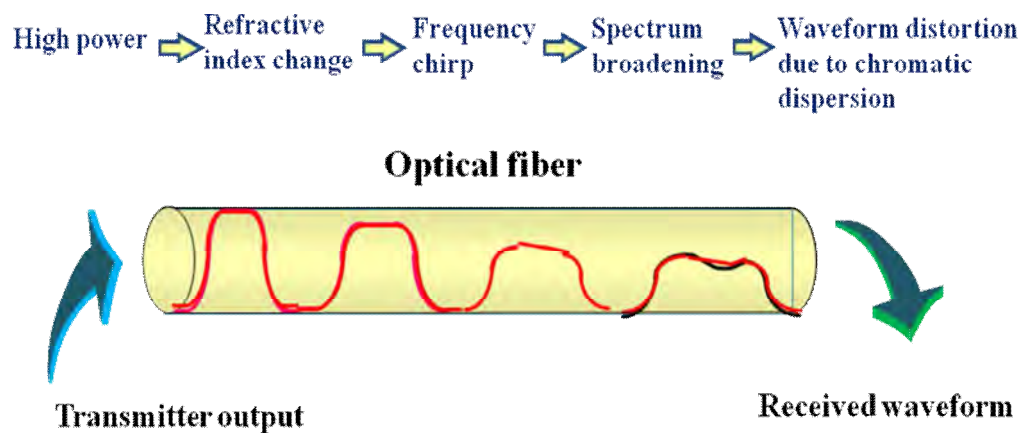
Fig.2.2: Waveform distortion due to dispersion effect

2.2.2 Nonlinear Impairments

When the optical communication systems operated at higher bitrates such as 10 Gbp/s and above and/or at higher transmitter powers, it is important to consider the effects of nonlinearities. In the case of WDM systems, nonlinear effects can become important even at moderate powers and bitrates. The nonlinear effects that we consider in this section arise owing to the dependence of the refractive index on the intensity of the applied electric field, which in turn is proportional to the square of the field amplitude. At sufficiently high optical intensities, non-linear refraction occurs in the core (Kerr effect), which is the variation of the index of refraction with light intensity. This makes

Nonlinear Impairments a critical concern in optical networks since long-haul transmission commonly relies on high power lasers to transmit optical pulses over long spans to overcome attenuation. Nonlinear impairments are comprised of interchannel and intrachannel nonlinearities. These impairments depend mainly on the fiber type and length and can be placed into two categories. The nonlinear effects that affect the shape of an optical pulse are

i) Self-Phase Modulation (SPM)
ii) Cross-Phase Modulation (XPM)

Secondly the nonlinear effects that affect the energy of an optical pulse are

i) Stimulated Brillouin Scattering (SBS)
ii) Stimulated Raman Scattering (SRS)
iii) Four-wave mixing (FWM)

Fig.2.3: Nonlinear effects in optical fiber

2.2.2.1 Inter-Channel Nonlinearities

There are three types of fiber nonlinearities due to the Kerr effect. Type (i) self phase modulation (SPM) (ii) cross phase modulation (XPM), and (iii) four wave mixing (FWM).

i) Self-Phase Modulation (SPM)

Self-phase modulation (SPM) is due to the power dependence of the refractive index of the fiber core. SPM refers the self-induced phase shift expe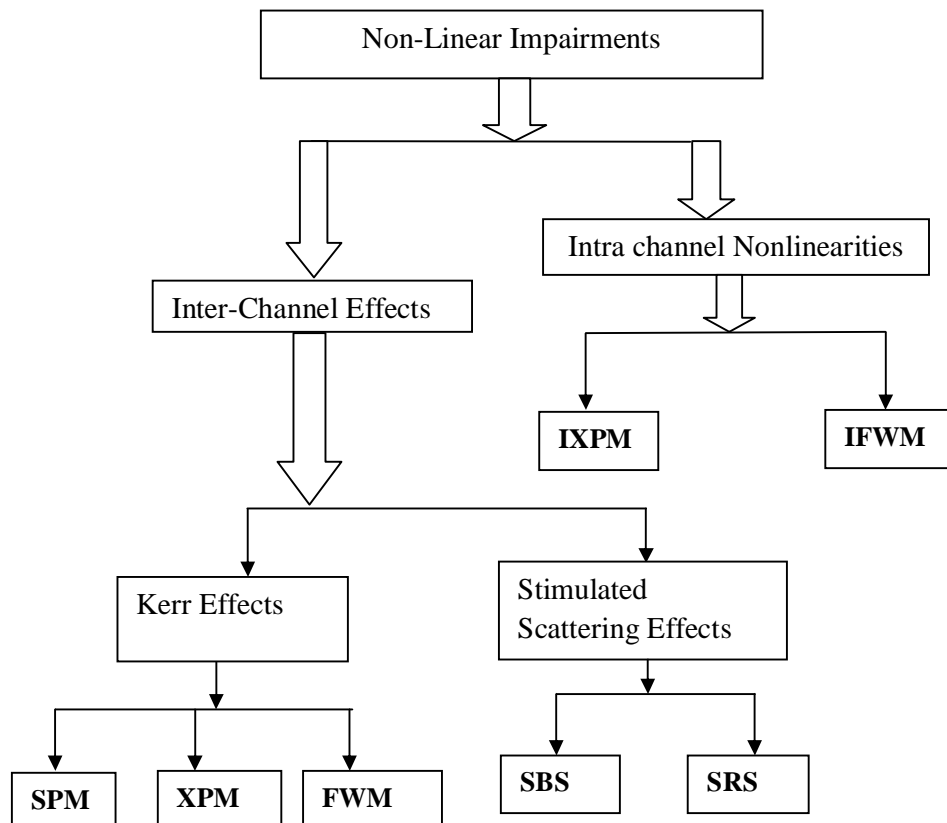rienced by an optical field during its propagation through the optical fiber; change of phase shift of an optical field is given by

$$\phi(z,\tau) = \left(\frac{2\pi}{\lambda} n_0 z + \frac{2\pi}{\lambda} n_2 |E|^2 z_{eff} \right) = \phi_L + \phi_{NL} \tag{2.10}$$

Here $k_0 = \dfrac{2\pi}{\lambda}$ and E is the electric field of the transmitted pulse, ϕ_L is the linear part and ϕ_{NL} is the nonlinear part that depends on intensity. Here z_{eff} is the effective transmission distance taking into account of the fiber attenuation, and it is given by

$$z_{eff} = \frac{1 - e^{-\alpha z}}{\alpha}$$

The first term in Eqn. (2.10) is just a linear phase shift, and depends only on the transmission distance z. On the other hand, the second term in (2.10) depends not only on the transmission distance z by way of z_{eff}, but also the intensity variation of the signal E itself. Therefore, this effect is called self phase modulation (SPM). The intensity dependence of refractive index causes a nonlinear phase shift, which is proportional to the intensity of the signal. It should be noted that z_{eff} is less than z . This implies that fiber attenuation reduces the effect of nonlinear phase shift. SPM alone broadens the signal spectrum, but does not affect the intensity profile of the signal. The spectral broadening effect can be understood from the fact that the time-dependent phase variation causes instantaneous frequency deviation $\delta\omega(\tau)$, which is given by

$$\delta\omega(\tau) = -\frac{\partial\varphi}{\partial\tau} = \frac{2\pi n_2 z_{eff}}{\lambda} \frac{\partial E(\tau)}{\partial\tau} \tag{2.11}$$

Eqn. (2.11) suggests that the magnitude of instantaneous frequency deviation increases with distance and the intensity variation of the signal. Thus different parts of the pulse undergo a different phase shift, which gives rise to chirping of the pulses. The SPM-induced chirp affects the pulse broadening effects of dispersion. The spectrum broadening effect caused by SPM may result in inter-channel cross talk among channels in WDM systems. The combined effect of dispersion and SPM strongly depends on the sign of dispersion (the sign of D). In terms of the sign of dispersion, the operating wavelength region is divided into two regimes: normal dispersion and anomalous dispersion regimes. The normal dispersion regime corresponds to the wavelength range in which dispersion D is negative (β_2 is positive) whereas the anomalous dispersion regime is the wavelength region in which D is positive (β_2 is negative). For the propagation of an optical pulse, the SPM enhances the effect of dispersion when the operating wavelength is in the normal dispersion regime. That is, the pulse is broadened more severely than under the effect of dispersion alone in the normal dispersion regime.

ii) Cross Phase Modulation (XPM)

Cross phase modulation (XPM) is very similar to SPM except that it involves two pulses of light, whereas SPM needs only one pulse. In Multi-channel WDM systems, all the other interfering channels also modulate the refractive index of the channel under consideration, and therefore its phase. This effect is called XPM. XPM refers the nonlinear phase shift of an optical field induced by co-propagating channels at different wavelengths; the nonlinear phase shift be given as

$$\phi_{NL} = n_2 k_0 L \left(\left| E_1 \right|^2 + 2 \left| E_2 \right|^2 \right)$$

where E_1 and E_2 are the electric fields of two optical waves propagating through the same fiber. In XPM, two pulses travel down the fiber, each changing the refractive index as the optical power varies. If these two pulses happen to overlap, they will introduce distortion into the other pulses through XPM. Unlike, SPM, fiber dispersion has little impact on XPM. Increasing the fiber effective area will improve XPM and all other fiber nonlinearities.

iii) Four-Wave Mixing (FWM)

The intensity dependence of refractive index not only causes nonlinear phase shift but also gives rise to the process by which signals at different wavelengths are mixed

together producing new signals at new wavelengths. This process is known as four-wave mixing (FWM). The processes (SPM and XPM) causing the nonlinear phase shift but energy transfer occurs in the FWM process. When signals at frequencies f_i, f_j; and f_k propagate along an optical fiber, the nonlinear interactions among those signals by mean of FWM result in the generation of new signals at

$$f_{ijk} = f_i + f_j - f_k$$

The energies from the interacting signals are transferred to those newly-generated signals at frequencies f_{ijk}. In the simplest case when only two signals at frequencies f_1 and f_2 are involved, the FWM generates new signals at $2 f_1 - f_2$ and $2 f_2 - f_1$ as demonstrated in Fig. 2.4. The number of FWM-generated signals grows rapidly with the number of involved signals
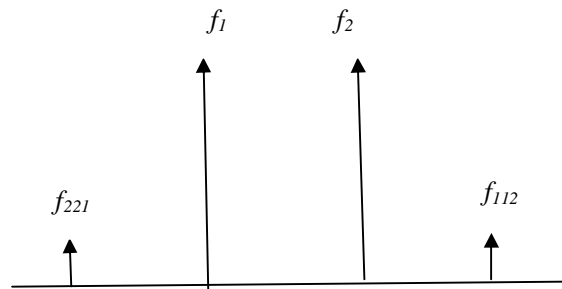
Fig. 2.4: Illustrations of FWM process of two signals at frequencies f_1 and f_2

When N signals are involved in the FWM process, the number of FWM generated signals is given by

$$M = \frac{N^2(N-1)}{2}$$

For example, when 10 signals are four-wave mixed together, 450 signals are generated. In WDM systems, not only does the FWM cause power depletion on the participating channels, but it also results in cross talk among channels. The cross talk comes from the fact that some of the FWM-generated signals can have the same frequencies as the WDM channels when all channels are equally spaced in frequency. For a single carrier systems, when the pulse have strong broadening due to chromatic dispersion, the nonlinear mixing of overlapped pulses generates ghost pulses in neighboring time slots due to intra-channel four wave mixing fiber optic system (IFWM), which is one of the

dominant penalties for high bit rate (above 40 Gb/s) . The difference between FWM and IFWM is that echo pulses appear in time domain instead of in frequency domain.

iv) Stimulated Brillouin Scattering (SBS)

In the stimulated scattering processes, the optical fiber acts as a nonlinear medium and plays an active role through the participation of molecular vibrations. When a powerful light wave travels through a fiber it interacts with acoustical vibration modes in the glass. This causes a scattering mechanism to be formed that reflects much of the light back to the source. SBS corresponds to the interaction of the optical waves with the acoustic waves that occur in the fiber. A contra directional scattering at frequencies smaller than the incident frequency takes place. The threshold of this non-linear effect depends on the source spectral width and on the power density in the fiber.

The SBS threshold power is given by Y. Aoki, et al. [23] is:

$$P_{thr} = \frac{21A_{eff}}{g_B L_{eff}}\left[1 + \frac{\Delta v_p}{\Delta v_B}\right]$$

Where Δv_p and Δv_B are the line-widths of the input laser and the Brillouin line, A_{eff} and L_{eff} are the effective core area and the effective length of the fiber, and g_B is the Brillouin gain in the fiber.

v) Stimulated Raman Scattering (SRS)

If two or more signals at different wavelengths are injected into a fiber, SRS causes power to be transmitted from lower wavelength channels to the higher wavelength channels. The incident light interacts with the molecular vibrations in a fiber and scattered light is generated, down-shifted by the Stokes frequency. The magnitude of the peak gain coefficient scales inversely with the pump wavelength. For a single injected channel, the amplification of spontaneous Raman scattered light can cause depletion of the signal light. In general, the criterion used to determine the level of scattering effects is the threshold power P_{th} defined as the input power level that can induce the scattering effect so that half of the power (3-dB power reduction) is lost at the output of an optical fiber of length z. The threshold power P_{th} is given by

$$P_{th} = \frac{32\alpha A_{eff}}{g_R}$$

where α and A_{eff} are the attenuation coefficient and effective core area of an optical fiber, respectively, and g_R is the Raman gain coefficient. For a 1.55-μm single channel system employing a standard single-mode optical fiber, P_{th} is found to be of the order of 1 W. Commonly, the transmitted power is well below 1 W; thus, the effect of SRS is negligible in single-channel systems.

The effect of Raman scattering is different when two or more signals travel along an optical fiber. When two optical signals separated by the Stokes frequency travel along an optical fiber, the SRS would result in the energy transfer from the higher frequency signal to the lower frequency signal. That is, one signal experiences excess loss whereas another signal gets amplified. The signal that is amplified is called the probe signal whereas the signal that suffers excess loss is called the pump signal. The effectiveness of the energy transfer depends on the frequency difference (Stokes frequency) between the pump and probe signals.

2.2.2.2 Intra-Channel Nonlinearities:
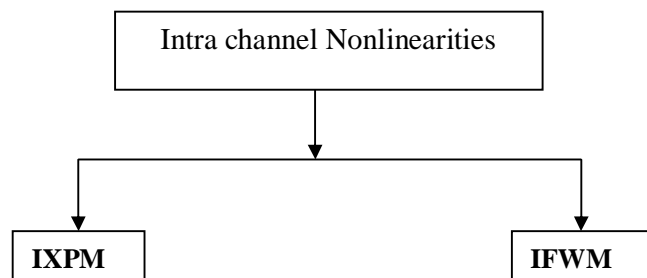
Fig.2.5: Intra-channel nonlinear effects in optical fiber

i) Intra-Channel Cross Phase Modulation

IXPM is a pulse to pulse effect within a channel, which occur only when the pulses overlap in time during their propagation. It is a phase perturbation that occurs to a specified pulse, resulting from the phase of neighboring pulses, in the same channel. In OOK systems, phase modulation changes the frequency of the pulse which results in timing jitter. In PSK systems it introduces phase modulation resulting in phase variation. Since the data encoding of PSK system is based on the phase difference between subsequent bits, therefore, phase variation could possibly distort the signal. The simplest way to demonstrate the effect of IXPM is by considering propagation of a

single pair pulses. The equation of propagation describing the effect of SPM and IXPM on each pulse pair can be obtained by

$$\frac{\partial B_n}{\partial z} + \frac{i}{2}\beta_{3-n}(z)\frac{\partial^2 B_n}{\partial t^2} = iS(z)\gamma|B_n|^2 B_n + 2iS(z)\gamma|B_{3-n}|^2 B_n \qquad (2.12)$$

Where we normalized the pulse amplitude A_n to

$$B_n = A_n \exp[{}^{l(z)}\!\!\diagup\!\!{}_2]$$

Where $n= 1, 2$ and $S(z)= \exp[{}^{l(z)}\!\!\diagup\!\!{}_2]$ is the power evolution. Here γ is the nonlinear coefficient and the second term of equation (2.12) represents the effect of cross-phase modulation of one pulse on another and is the IXPM effect (Fig.2.6).
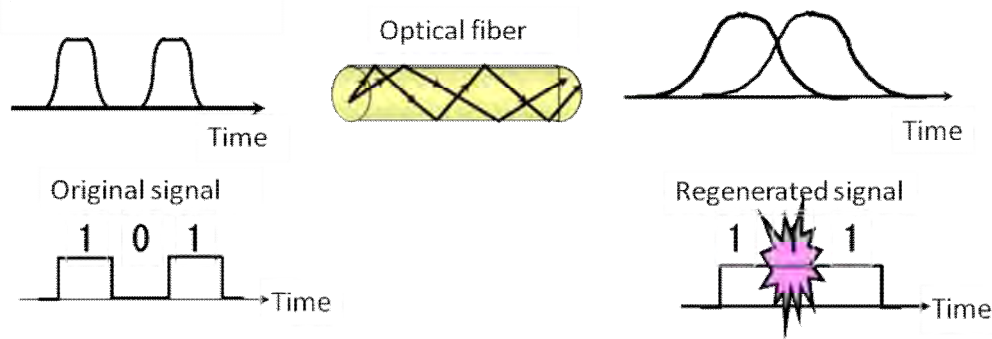
Fig.2.6: Signal distortion due to IXPM in optical fiber

If the dispersion is sufficiently low, there is an overlapping of the trailing edge of the first pulse with the leading edge of second pulse In this case, the pulses overlap in the regions where the slope of power is strong, resulting a large frequency shift. In the case of high dispersion, the pulses experience a strong broadening and their power slope is low. As a result, IXPM induced chirp is weak. A more significant effect of IXPM is the generation of timing jitter through the frequency shifts that are converted into time shifts by dispersion.

ii) Intra-Channel Four Wave Mixing

In contrast to IXPM, IFWM causes the transference of energy among the interacting pulses. In particular; this phenomenon can create new pulses in the time domain, which

are usually referred to as ghost pulses. These pulses were observed for the first time in 1992 in the context of an experiment involving a pair of ultra short pulses. IFWM ghost pulses interfere with neighboring pulses, because the level of zero bits to increase and the amplitude of one bit to fluctuate. In quasilinear systems, IFWM-induced ghost pulses introduce extra eye closure to the signal, which is only caused by fiber attenuation, α and inter-symbol interference (ISI) in linear systems.

As for study of IFWM, let us study the interaction in a pulse pair. Assuming that the optical field of pulse pair after transmission is *B(z,t)* which can be written as

$$B(z,t) = \sum_{1}^{2} B_n(z,t) + \Delta B(z,t)$$

Where $B_n(z,t)$ is the dispersive pulse evolution and $\Delta B(z,t)$ is the perturbed field from nonlinear interaction assuming $\left| \Delta B \right| << \left| B_{1,2} \right|$.

The equation of evolution of $\Delta B(z,t)$ can be written as,

$$\frac{\partial \Delta B}{\partial z} + \frac{i}{2} \beta_2 \frac{\partial^2 \Delta B}{\partial t^2} = iS(z)\gamma \sum_{m,n,p=1}^{2} B_m B_n^* B_p$$

Where *S(z)* is the power evolution along the line normalized to the transmission fiber. *β*$_2$ is the second order dispersion (GVD) coefficient. *γ(z)* presents the Kerr nonlinear coefficient and *m , n, p* are the labeling individual pulses.

In Dispersion Shifted Fiber (DSF), when 1550 nm wavelength is considered, there is no performance degradation due to IFWM. This can be easily understood because no pulse overlapping is experienced. In NZDSF, (*D*=4 ps/nm/km) IFWM effect is noticeable when the accumulated dispersion increases, but after one point, its increment rate reduces, and after a long distance of transmission, no more increment can be noticed. However, in comparison to the combined effect of IXPM and ISPM, IFWM effect is considered insignificant for highly dispersive fiber [18].

2.3 Why Working with IXPM?

The introduction of WDM with optical amplifiers has revolutionized the optical fiber transmission system by increasing the system capacity both by the number of channels and distance. Transmission capacity can be further enhanced by increasing the channel bit rate. The channel bit rate is upgraded to 40 Gb/s from

10 Gb/s and it is predicting that the next generation light wave communications will be based on 80 Gb/s rate or even more. The effect of dispersions, non-linearities and fiber losses increase with increasing the capacity of optical fibers. This high bit rate systems will face many problems due to fiber dispersion and nonlinearity which are interrelated with transmitting power, number of channels, channel spacing and transmission length etc. The IXPM effect still may be in a tolerable limit at current bit rate of optical fiber transmission scheme but its effect is increasing with the increasing bit rate. This is because of the increase in intra-channel collision between consecutive pulses due to enhanced bit rate. That's why IXPM has become a concern now a day in dispersion management system. This fact has motivated us in this research. For this reason, intra-channel cross phase modulation induced phase fluctuations in a periodically dispersion managed transmission is the main focus of our thesis.

2.4 Conclusion

This chapter briefly discuss about impairments of optical fiber. The physical impairments of optical fiber transmission can be categorized into two main parts irrespective of modulation/detection schemes: linear and nonlinear. Linear barriers include fiber loss and dispersion, on the other hand nonlinear part comprises inter-channel and intra-channel impairments. Inter-channel impairments are SPM, XPM, and FWM. On the other hand, intra-channel cross-phase modulation (IXPM) and intra-channel four-wave mixing (IFWM) are the dominating intra-channel nonlinearities. These nonlinearities are realized to be the major performance limiting factor for phase modulated light wave communication systems.

CHAPTER 3
THEORITICAL ANALYSIS OF IXPM INDUCED PHASE FLUCTUATIONS

3.1 Introduction

IXPM is one of the crucial nonlinear impairments in single channel lightwave systems. It causes phase fluctuations of intra-channel pulses and also detrimental for phase sensitive modulation formats. As SPM-induced phase fluctuations are deleterious for single channel transmission, however, IXPM-induced phase fluctuations are much concern for optical transmission [18]. Since we are considering dispersion management system with highly dispersive fibers like standard single mode fiber and dispersion compensating fiber, the effect of IFWM is considered negligible here. In this Chapter, the basic theories and fundamental equations of optical pulse propagation in a fiber have been studied. We have explored the dynamics of pulse-to-pulse collisions in a single-channel system and the influence of IXPM on phase fluctuation of RZ pulse. Here, we use variational method to examine the collision-induced phase shift analytically and numerical analysis split-step Fourier method is utilized to validate the analytical results.

Section 3.2 introduces the fundamental equation that describes the propagation of an optical pulse within the optical fiber. The elementary equation of light wave propagation can be derived from Maxwell's equation and can be transformed into nonlinear Schrödinger (NLS) equation. Section 3.3 describes variational analysis for a single-channel dispersion management system. For checking the results of analytic techniques, we have introduced a numerical technique known as Split Step Fourier Method (SSFM). This is discussed in section 3.4. Finally Section 3.5 states the periodic dispersion management techniques.

3.2 Elementary Equation of Light wave Propagation

The complex envelope of a slowly varying optical field propagating in a fiber can be described by the following equation, which is derived from Maxwell's equation by using reductive perturbation method and making some assumptions as,

$$i\left\{\frac{\partial E}{\partial z} + \beta_1(z)\frac{\partial E}{\partial t}\right\} - \frac{\beta_2(z)}{2}\frac{\partial^2 E}{\partial t^2} + \gamma(z)|E|^2 E = -ig(z)E, \qquad (3.1)$$

where $E(z, t)$, z and t are the complex electric field, propagation distance and time, in real world units, respectively. $\beta_1(z)$ is the inverse of group velocity and $\beta_2(z)$ is the group velocity dispersion (GVD), $\gamma(z)$ presents the Kerr nonlinear coefficient, which is related to nonlinear refractive index of fiber n_2 and its effective core area A_{eff} by $\gamma = \frac{2\pi n_2}{\lambda A_{eff}}$, where λ is the wavelength of light. $g(z)$ represents the fiber loss if $g(z) < 0$ or gain if $g(z) > 0$. For fiber with loss α [dB/km], $g(z)$ is expressed as $g(Z) = \alpha \times \log_e(10\!/\!20)$, Using chain rule and introducing new time coordinate $\tau = t - \int_0^z \beta_1(\zeta)d\zeta$, we can derive the following equation

$$i\frac{\partial E}{\partial z} - \frac{\beta_2}{2}\frac{\partial^2 E}{\partial \tau^2} + \gamma(z)|E|^2 E = -ig(z)E. \qquad (3.2)$$

Next we introduce new non-dimensional variables as follows:

$$T = \frac{\tau}{t_0}, \quad Z = \frac{z}{z_0}, and \quad u = \frac{E}{\sqrt{P_0}}$$

where t_0, z_0 and P_0 are the arbitrary constants in real units for normalizing the quantities that describe the time, distance and electric field for optical signal, respectively. Now we can achieve the normalized form of Eq. (3.1) as follows

$$i\frac{\partial u}{\partial Z} - \frac{b(Z)}{2}\frac{\partial^2 u}{\partial T^2} + s(z)|u|^2 u = -i\Gamma(Z)u,$$

where $b(Z)$, $s(Z)$ and $\Gamma(Z)$ indicate the dispersion profile, the fiber nonlinearity and loss in normalized form, respectively and these normalized quantities are denoted as

$$b(Z) = \frac{\beta_2 z_0}{t_0^2}, s(Z) = \gamma(Z)z_0 P_0, \quad \Gamma(Z) = g(Z)z_0$$

In actual optical fiber communication systems, fiber amplifiers, either lumped or distributed, are periodically installed along the transmission line to compensate for the loss between two successive amplifiers. Pulse envelope will change periodically due to

this periodic amplification. We use the transformation $u(Z,T)= a(Z)U(Z,T)$, where $U(Z, T)$ is a slowly varying amplitude of pulse envelope and $a(Z)$ is a rapidly varying term, which is a periodic real function with period of amplifier spacing can be given by

$$a(Z) = a_0 \exp\left\{\int_0^Z \Gamma(Z^{'})dZ^{'}\right\},$$

where a_0 is a constant determined by the gain of amplifier and calculated as

$$a_0 = \sqrt{\frac{2\Gamma Z_0}{1-\exp(-2\Gamma Z_a)}},$$

here Γ is fiber loss and Z_a is amplifier spacing, both are in normalized units. We obtain the following equation after the transformation

$$i\frac{\partial U}{\partial Z} - \frac{b(Z)}{2}\frac{\partial^2 U}{\partial T^2} + S(Z)|U|^2 U = 0, \tag{3.3}$$

where $S(Z)$ represents the normalized effective fiber nonlinearity, which includes the effect of fiber nonlinearity, fiber loss and periodic gain. We can apply this equation in a system with periodic dispersion compensation while retaining periodic or constant nonlinearity. If fiber dispersion and nonlinearity are kept constant and fiber is lossless, $b(Z)$ and $S(Z)$ can be normalized to unity, then Eq. (3.3) can be written as

$$i\frac{\partial U}{\partial Z} - \frac{1}{2}\frac{\partial^2 U}{\partial T^2} + |U|^2 U = 0. \tag{3.4}$$

This is the well known nonlinear Schrödinger (NLS) equation with constant coefficients, the basic equation for optical soliton, which is integrable and can be solved analytically. The fundamental stationary solution of Eq. (3.4) is known as solitary wave (soliton) solution which is given by

$$U(Z,T) = \eta \operatorname{sech}\{ T + kZ - T_0(Z)\} \exp\left[-ikT + \frac{i}{2}(\eta^2 - k^2)Z + i\theta_0\right]. \tag{3.5}$$

Here η represents the amplitude as well as pulse width of soliton, κ represents its speed which indicates the deviation from the group velocity as well as the

frequency. T_0 and θ_0 represent the initial center position of soliton pulse in time and initial phase, respectively.

When $b(Z)$ and/or $S(Z)$ is not constant with respect to Z, Eq. (3.3) is termed as NLS equation with varying coefficients, and it is no longer integrable. It implies that we cannot find any exact solution, but we can obtain an approximate analytical solution.

3.3 Analytical Calculation of IXPM-Induced Phase Shift

As we have mentioned in previous sub-section, Eq. (3.3) cannot be solved analytically. Several methods have been developed to explain and to study the propagation of nonlinear return-to-zero stationary pulse under those conditions: the perturbation theory [22], the guiding center theory [23], the variational method [24], and the numerical averaging method [25] etc. The fundamental nature of these methods is to reduce the original perturbed system with dispersion management into a simpler model or an approximate equation is assumed which can be easily solved. The methods provide us a way to explore the characteristics of DM soliton considering some perturbations. In this thesis, considering a known function for the solution of pulse waveform, we study the variational method to examine the attributes and evolution of pulse in fiber-optic transmission line with periodic dispersion compensation and amplification. We also accomplish direct numerical calculations of the perturbed NLS equation to analyze the evolutionary properties and verify our variational results. Optical pulse propagation in fiber described by the NLS equation with periodically varying effects and small perturbations can be written as

$$i\frac{\partial U}{\partial Z} - \frac{b(Z)}{2}\frac{\partial^2 U}{\partial T^2} + \gamma(Z)|U|^2 U = R(Z,T), \tag{3.6}$$

here $\gamma(Z)$ is the fiber non-linearity and $R(T, Z)$ represents the perturbation term and R<<1. As pulse is impaired by the perturbation $R(Z, T)$, it is essential to examine the dynamics of pulse amplitude, width, chirp, frequency, position and phase under the influence of perturbation. We use the variational method to investigate the pulse dynamics with the perturbation. The dynamics of optical pulse, $U(Z, T)$, in dispersion managed optical communication system can be described by nonlinear Schrödinger equation (NLSE):

$$i\frac{\partial U_j}{\partial Z}+\frac{D(Z)}{2}\frac{\partial^2 U_j}{\partial T^2}+\gamma(Z)\left|U_j\right|^2 U_j=-2\gamma(Z)\left|U_{3-j}\right|^2 U_j,\tag{3.7}$$

Where U is the slowly varying envelop of the pulse, $D(z)$ and $\gamma(z)$ represent dispersion and nonlinear coefficients respectively, T and Z are normalized retarded time and propagation distance. Here we assume that interactions between adjacent two RZ pulses, ($j=1, 2$), are only due to IXPM. Substituting to NLSE and ignoring other nonlinear effects except self phase modulation (SPM) and IXPM, we assume that the solution of Eq. (3.7) can be approximated by a Gaussian pulse associated with linear chirp as

$$U_j(Z,T)=A_j(Z)f(\tau_j)\exp(i\phi_j),\tag{3.8}$$

$$\tau_j=p_j\left(T-T_j\right),$$

$$\phi_j=(\frac{C_j}{2})\tau_j^2-\left(\frac{\kappa_j}{p_j}\right)\tau_j+\theta_J,$$

where $A(Z), p(Z), C(Z), \kappa(Z), T_0(Z)$ and $\theta(Z)$ are the six pulse parameters representing the j-th pulse's amplitude, the inverse of pulse width, the linear chirp, the central frequency, the central time position and the phase of the pulse, respectively. The pulse propagating in a dispersion-managed system has almost Gaussian shape and we can then assume the Gaussian pulse,

$$f(\tau_j)=\exp(\frac{-\tau_j^2}{2}),$$

the approximate solution becomes

$$U(Z,T)=A_j\exp[-\frac{1}{2}(1-iC_j)\tau_j^2-i\frac{\kappa_j}{p_j}\tau+i\theta_j].$$

Applying variational method [24] to Eqn. (3.7), the dynamical equations of these parameters under perturbation can be derived as

$$\frac{dp_j}{dZ}=-D(Z)p_j^3 C_j,\tag{3.9}$$

$$\frac{dC_j}{dZ} = D(Z)p_j^2(1+C_j^2) - \gamma(Z)\frac{E_j p_j}{\sqrt{2\pi}} - 4E_{3-j}p_{3-j}^2\{P^2 - 2(\Delta\tau)^2\}K, \tag{3.10}$$

$$\frac{d(\Delta\kappa)}{dZ} = 4(E_1 + E_2)p_1 p_2 P^2(\Delta\tau)K, \tag{3.11}$$

$$\frac{d(\Delta\tau)}{dZ} = -D(Z)\{\Delta\tau\sum_{j=1}^{2} p_j^2 C_j + p_1 p_2 \Delta\kappa\}, \tag{3.12}$$

$$\frac{d\theta}{dZ} = \frac{D(Z)}{2}\left(\kappa_j^2 - p_j^2\right) + \gamma(Z)\frac{5E_j}{4\sqrt{2\pi}} p_j + E_{3-j}\left[2P^4 + p_{3-j}^2\{P^2 - 2(\Delta\tau)^2\}\right]K \tag{3.13}$$

here $\Delta\kappa = \kappa_1 - \kappa_2$,

$$P = \sqrt{(p_1^2 + p_2^2)},$$

$$\Delta\tau = p_1 p_2 (T_1 - T_2),$$

$$K = \frac{\gamma(Z)}{\sqrt{\pi}}\frac{p_1 p_2}{P^5}\exp\{-(\frac{\Delta\tau}{P})^2\},$$

here $E_j = \sqrt{\pi}A_j^2\big/p_j$ is constant representing pulse energy of U_j.

Since $\kappa_1(0) = \kappa_2(0) = 0$,

$E_1\kappa_1 + E_2\kappa_2 = 0$ is satisfied for any Z and representing the conservation of momentum.

The pulse phase can be evaluated by,

$$\theta_j(Z) = \theta_j(0) + \frac{1}{2}\int_0^Z D(\zeta)(\kappa_j^2(\zeta) - p_j^2(\zeta))d\zeta$$

$$+ \frac{5E_j}{4\sqrt{2\pi}}\int_0^Z \gamma(\zeta)p_j(\zeta)d\zeta + E_{3-j}\int_0^Z \left[2P^4 + p_{3-j}^2\{P^2 - 2(\Delta\tau)^2\}\right]K(\zeta)d\zeta, \tag{3.14}$$

where

$$\theta_{Disp}(Z) = \frac{1}{2}\int_0^Z D(\zeta)(\kappa_j^2(\zeta) - p_j^2(\zeta))d\zeta,$$

$$\theta_{SPM}(Z) = \frac{5E_j}{4\sqrt{2\pi}}\int_0^z \gamma(\zeta)p_j(\zeta)d\zeta,$$

$$\theta_{XPM}(Z) = E_{3-j}\int_0^Z \left[2P^4 + p_{3-j}^2\left\{P^2 - 2(\Delta\tau)^2\right\}\right]K(\zeta)d\zeta.$$

Here $\theta_j(0)$ indicates the initial pulse phase. θ_{Disp}, θ_{SPM} and θ_{XPM} terms imply the contributions from dispersion, SPM, and XPM, respectively. The phase shift observed at any channel is deduced as

$$\delta\theta = \theta_2 - \theta_1, \tag{3.15}$$

where θ_2 is the observed phase when two pulses are transmitted through a single channel and θ_1 is the phase when single pulse is transmitted. Solving eqns. (3.9-3.13) by Runge-Kutta method and substituting the obtained values into Eq. (3.14-3.15), we can evaluate phase shift due to IXPM.

3.4 Numerical Calculation of IXPM-Induced Phase Fluctuation

Split step Fourier method (SSFM) is used as the numerical tool to calculate the IXPM induced Phase Fluctuation. The phase is calculated at the peak power of every pulse while propagation through the fiber. Next the calculated phase is plotted against different parameters. Split step Fourier method (SSFM) is used to simulate self phase modulation and chromatic dispersion in fiber optical communication simultaneously. The non-linear Schrödinger equation is described as

$$\frac{\partial U}{\partial z} = -i\frac{b(z)}{2}\frac{\partial^2 U}{\partial t^2} + i\gamma|U|^2 U = [\hat{D} + \hat{N}]U,$$

here $U(t,z)$ describes the pulse envelope in time t at the spatial position z. The equation can be split into a linear part,

$$\frac{\partial U_D}{\partial z} = -i\frac{b(z)}{2}\frac{\partial^2 U}{\partial t^2} = [\hat{D}]U,$$

and the nonlinear part,

$$\frac{\partial U_N}{\partial z} = i\gamma |U|^2 U = [\hat{N}]U.$$

Both the linear and the nonlinear parts have analytical solutions, but the nonlinear Schrödinger equation containing both parts does not have a general analytical solution. However, if only a 'small' step *h is* taken along *z*, then the two parts can be treated separately with only a 'small' numerical error. One can therefore first take a small nonlinear step, using the analytical solution.

$$U_N(t, z+h) = \exp[i\gamma |U|^2 U]U(t, z)$$

The dispersion step has an analytical solution in the frequency domain, so it is first necessary to Fourier transform U_N using

$$\tilde{U}_N(\omega, z) = \int_{-\infty}^{\infty} U_N(t, z) \exp[i(\omega - \omega_0)t]dt,$$

where ω_0 is the center frequency of the pulse. It can be shown that using the above definition of the Fourier transform, the analytical solution to the linear step, commuted with the frequency domain solution for the nonlinear step *h* is,

$$\tilde{U}(\omega, z+h) = \exp\left[\frac{ib(z)}{2}(\omega - \omega_0)^2 h\right]\tilde{U}_N(\omega, z).$$

By taking the inverse Fourier transform of $\tilde{U}(\omega, z+h)$ one obtains $U(t, z+h)$; the pulse has thus been propagated a small step *h*. By repeating the above *N* times, the pulse can be propagated over a length of *Nh*. These steps are illustrated in Figure 3.1.

In iterative and symmetric split step fourier method the signal is propagated through half of the distance `*h´* with dispersion acting on it and then at middle of the distance nonlinearity acts on it and then in the remaining half of the distance dispersion acts on it again depicted in the Fig 3.1. The process is approximated by the following equation:

$$U(z+h, T) \approx \exp\left(\frac{h}{2}\hat{D}\right)\exp\left(\int_z^{z+h}\hat{N}(z')dz'\right)\exp\left(\frac{h}{2}\hat{D}\right)U(z, T)$$

In the case of an amplified optical communication link, for each span between amplifiers several iterations, according to the number of divisions `h´, have to be performed for the mitigation of nonlinearity and dispersion, leading to a very high complexity.
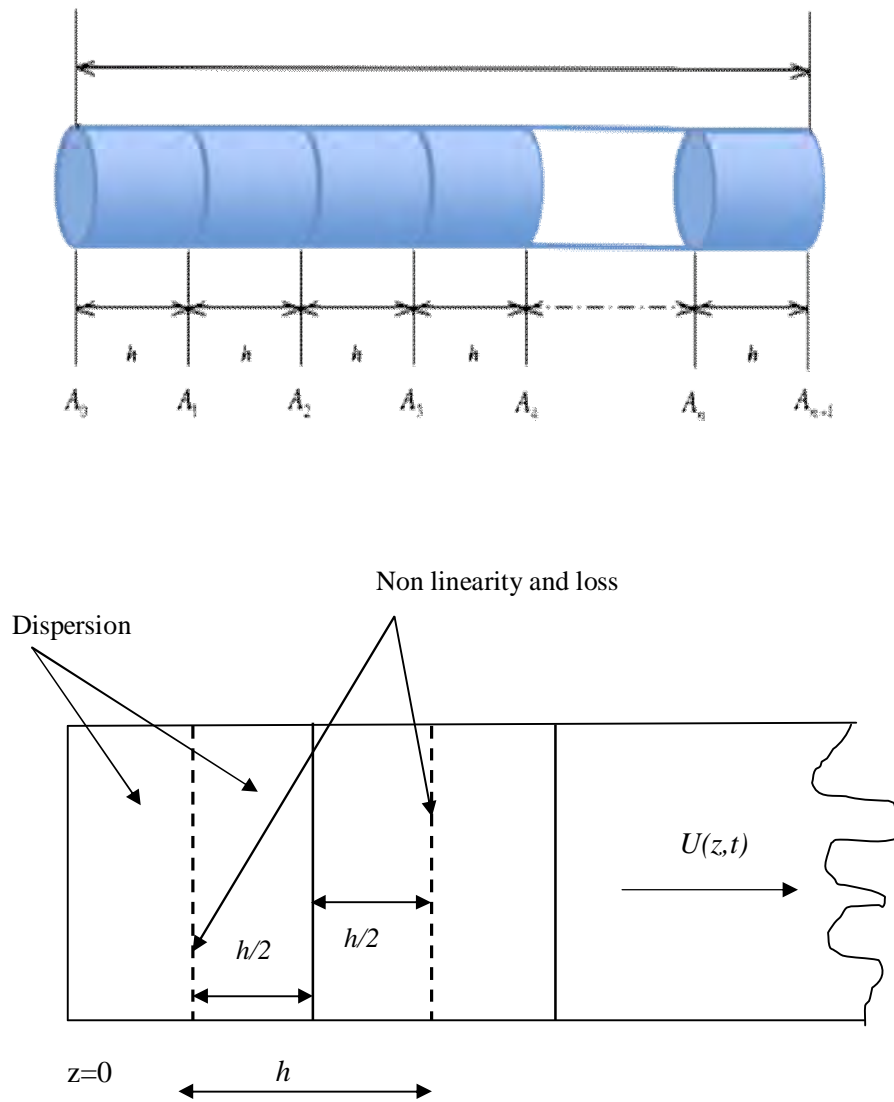

Figure 3.1: Illustration of symmetric split step Fourier method.

Flow Diagram of SSFM

```
┌─────────────────────────────────────────────────────┐
│          Generate Input Gaussian pulse,u             │
└─────────────────────────────────────────────────────┘
                          ↓
┌─────────────────────────────────────────────────────┐
│      Divide propagation Length into Discrete h Steps │
└─────────────────────────────────────────────────────┘
                          ↓
┌─────────────────────────────────────────────────────┐
│              Start from Position Z₀                   │
└─────────────────────────────────────────────────────┘
                          ↓
┌─────────────────────────────────────────────────────┐
│                   U:=FFT(u)                          │
└─────────────────────────────────────────────────────┘
                          ↓
┌─────────────────────────────────────────────────────┐
│   Apply linear step over h/2:  U:=U. exp(D.h / 2)    │
└─────────────────────────────────────────────────────┘
                          ↓
┌─────────────────────────────────────────────────────┐
│                   u:=IFFT{U}                          │
└─────────────────────────────────────────────────────┘
                          ↓
┌─────────────────────────────────────────────────────┐
│  Apply Non- linear step over h; n=−jγ|u|², u=u.exp(nh)│
└─────────────────────────────────────────────────────┘
                          ↓
┌─────────────────────────────────────────────────────┐
│                   U:=FFT(u)                          │
└─────────────────────────────────────────────────────┘
                          ↓
┌─────────────────────────────────────────────────────┐
│   Apply linear step over h/2:  U:=U. exp(D.h / 2)    │
└─────────────────────────────────────────────────────┘
                          ↓
                    ◇ Z₀= Z₀+h ◇
                          ↓
                    ( END )
```

Fig.3.2: Flow Diagram of Split Step Fourier method

Start from Position Z_0

U:=FFT(u)

Apply linear step over *h/2:* U:=U. exp($D.h / 2$)

u:=IFFT$\{U\}$

Apply Non- linear step over *h*; $n = -j\gamma |u|^2$, $u = u.\exp(nh)$

U:=FFT(u)

Apply linear step over *h/2:* U:=U. exp($D.h / 2$)

$Z_0 = Z_0 + h$

Until Fiber Length

END

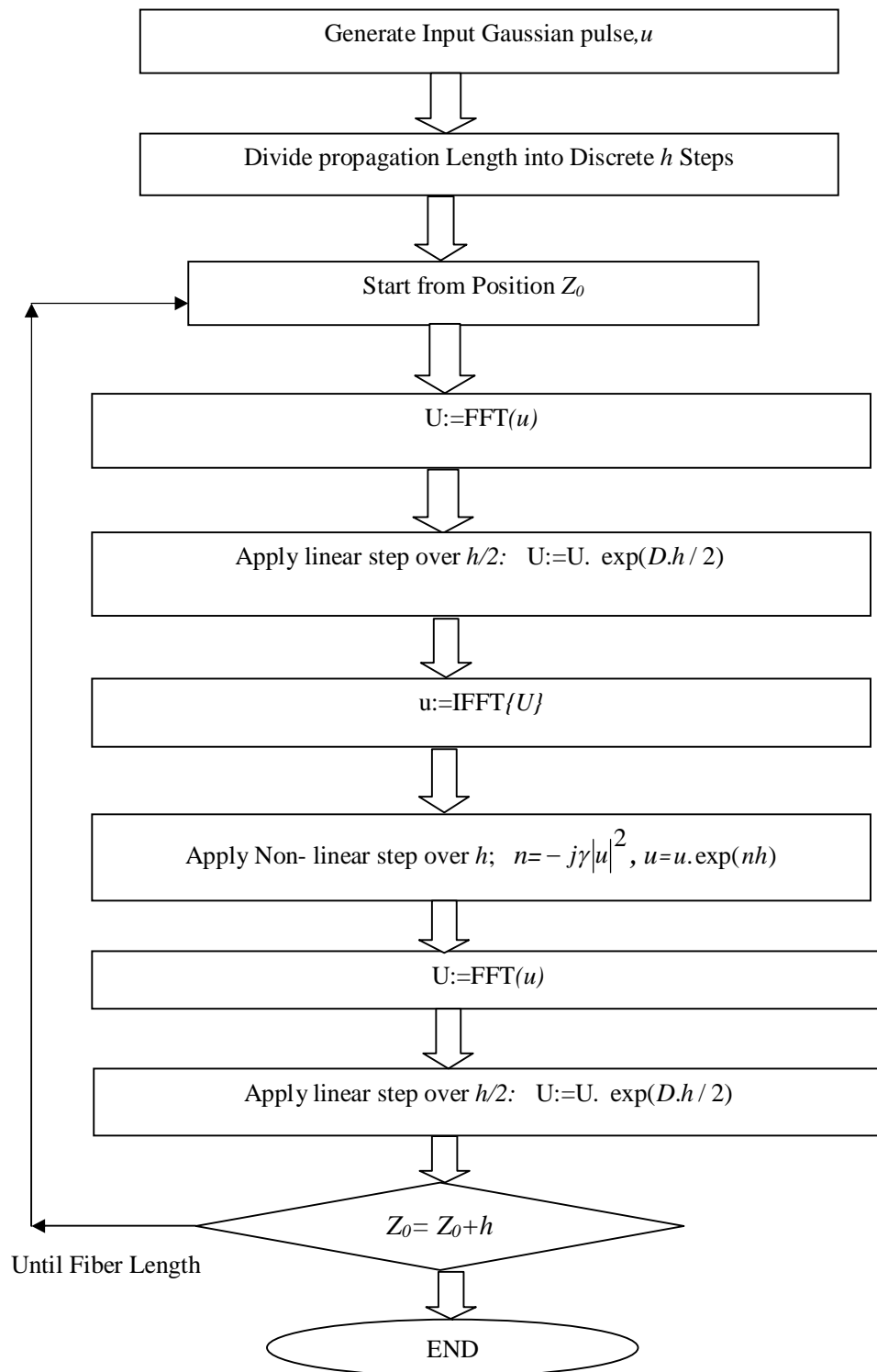Fig.3.2: Flow Diagram of Split Step Fourier method

3.5 Dispersion Compensation Techniques

In fiber optic communication systems, information is transmitted over the fiber by using a coded sequence of optical pulses, whose width is set by the bit rate B of the system. Dispersion induced broadening of pulses is undesirable as it interferes with the detection process, and it leads to errors if the pulse spreads outside its allocated bit slot ($T_B = 1/B$). The dispersion problem becomes quite serious when optical amplifiers are used to compensate for fiber losses because L can exceed thousands of kilometers for long-haul systems. A common method for managing dispersion is to combine two or more types of single-mode fiber to produce the desired dispersion over the entire link span. The total dispersion can be set at virtually any value as the contributions from different components may have opposite signs (i.e. either positive or negative) and hence they can partially, or completely, cancel each other. Dispersion-compensating fibers can be either placed at one location or distributed along the length of the fiber link.

Figure 3.3 shows a dispersion management scheme for a single-mode fiber link. It incorporates a dispersion management map to compensate positive dispersion (i.e. identified as D^+) on the fiber with the negative dispersion (i.e. identified as D^- such that the chromatic or total first-order dispersion D_r goes to zero.
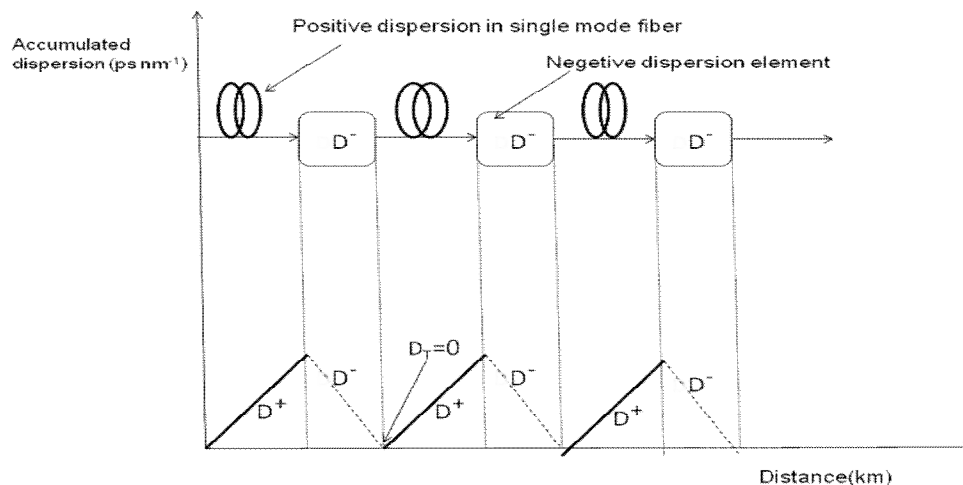

Fig. 3.3: Dispersion management scheme together with appropriate dispersion management map on a single-mode fiber-line

The implementation of fiber dispersion compensation can be done at the transmitter, at the receiver or within the fiber link. A typical transmission fiber (TF) consisted of the

standard single mode fiber (SSMF) with anomalous dispersion at 1550 nm and the DCF placed at the optical amplifier site within a double stage amplifier and it is shown in Fig 3.4. The use of DCF for dispersion compensation was first proposed in 1980, but due to the high loss of DCFs, this technique was not applied in practice until 1990s when the Erbium-doped fiber amplifier (EDFA) was presented.
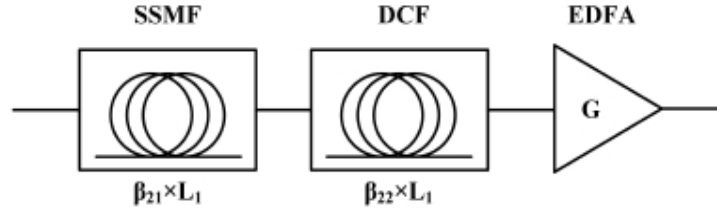
SSMF   **DCF**   **EDFA**

$\beta_{21} \times L_1$ $\beta_{22} \times L_1$

Fig. 3.4: A transmission span for DM system

If β_{21}, L_1 and β_{22}, L_2 are the GVD parameter and length for SSMF and DCF, respectively, then it can be shown that the total transfer function of SSMF cascades with a DCF is given by

$$H_{span}(\omega) = \exp\left[\frac{j\omega^2}{2}(\beta_{21}L_1 + \beta_{22}L_2)s(t)\right] \qquad (3.14)$$

It is evident from Eq. (3.14), that the perfect dispersion compensation is realized if

$$\beta_{21}L_1 + \beta_{22}L_2 = 0 \qquad (3.15)$$

Therefore, the optical pulses at the receiver are not broadened, and there is no ISI due to dispersion. Since β_{21} is negative (anomalous GVD) for standard fibers, therefore DCF must have normal dispersion $\beta_{22} > 0$, such that the accumulated dispersion in Eq. (3.15) becomes zero. The DCF with large positive value of GVD have been developed for the sole purpose of dispersion compensation in order to keep L_2 as small as possible. The use of DCFs provides an all-optical technique that is capable of overcoming the detrimental effects of chromatic dispersion (CD) in optical fibers provided the average signal power is low enough that the nonlinear effects remain negligible.

3.6 Conclusion

This chapter has explained the essential fundamental equation of an optical pulse propagating within a periodically varying dispersion management system. This equation is known as Non Linear Schrödinger Equation which can be derived from Maxwell's

equation by using so called reductive perturbation method. This chapter also presents a brief description of the two methods that we have used for the analysis of our thesis. The effect of IXPM is first seen by applying an analytic technique over basic pulse equation that is NLSE. This is done by well known variational method where we assume IXPM as a source of perturbation and derive the dynamical equations for pulse parameters. These pulse parameters are amplitude *(A)*, reciprocal of pulse width *(p)*, linear chirp *(C)*, central frequency *(κ)*, central time position *(T)* and the phase of the pulse *(θ)*. These ordinary differential equations have been solved by Runge-Kutta method to find out the phase fluctuations due to IXPM. Finally, split-step Fourier method (SSFM) is proposed to achieve the full numerical simulation to validate the accuracy of analytical model.

CHAPTER 4

IMPACT OF IXPM ON OPTICAL FIBER COMMUNICATION

4.1 Introduction

This chapter provides the summary of the results stating the significance of the parameters that could affect IXPM for different models. Results are obtained by applying variational method for analytical simulation and SSFM for numerical analysis. This chapter also gives the feedback of our research. The simulations are done in C code and then the output data files are plotted using MATLAB. In the section 4.2, a brief description of uncompensated single fiber transmission has been specified. The relation of IXPM induced phase fluctuation as a function of transmission distance; duty cycle and power for two types of single fiber transmission are focused in sub-section 4.2.1-4.2.5. In section 4.3, the system description of a single channel dispersion managed system is presented. The analytical and numerical results of our research related to DM system are described in section 4.3. The effects of various parameters on phase fluctuation such as transmission distance, input power, duty cycle, bit interval, bit-rate and dispersion map strength have been studied in sub-section 4.3.2-4.3.7. The amount of phase shift due to IXPM is also investigated for different DM transmission model system. Finally, section 4.4 gives the summary of the obtained results.

4.2 System Description of Uncompensated Single Fiber Transmission

We model a single channel system with a single fiber transmission. We theoretically analyze the pulse behavior along the transmission fiber. Transmission line with highly dispersive fibers like standard single mode fiber (SSMF) and Non-zero dispersion–shifted fiber (NZDSF) is considered for two different systems. We consider the total transmission period of around 100 km. Model parameters for SSMF is taken as dispersion parameter 17ps/nm/km, effective core area $80\mu m^2$ and nonlinear index coefficient $2.5\times10^{-20}m^2/W$. In another system, we use NZDSF in place of SSMF. It has fiber parameters as following: dispersion 4ps/nm/km, effective core area $50\mu m^2$ and

nonlinear index coefficient $1.5 \times 10^{-20} m^2/W$. We assumed bit rate of 40 Gb/s with peak power 1mW for each pulse with each of them having wavelength of 1.55µm. The minimum pulse width (FWHM) is taken as 10ps and the pulses have a difference in time domain of 25ps.
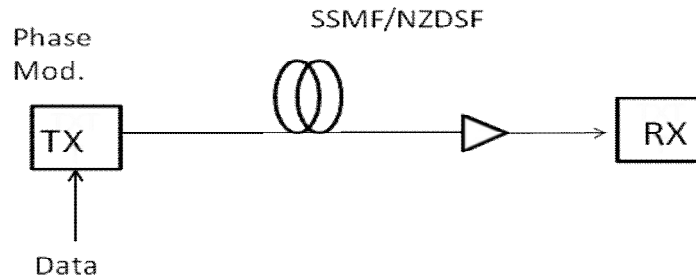

Fig 4.1: Uncompensated Single Fiber Transmission System using SSMF or NZDSF

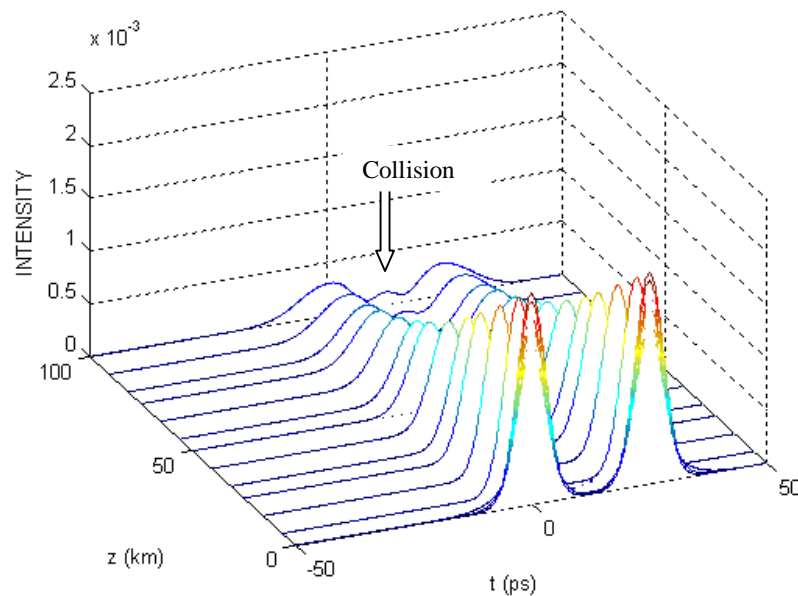## 4.2.1 Pulse Propagation in Uncompensated Transmission System

Fig.4.2: Pulse dynamics within uncompensated SSMF system with full numerical simulation

We numerically simulate the Gaussian pulse evolution in single fiber transmission system for a transmission period of 100 km. We show pulse evolution along SSMF in the absence of noise in Fig. 4.2. We observe stationary pulse propagation for two pulses. It is evident from Fig.4.2 that each pulse is spreading out as it propagates down the

fiber. Under the influence of dispersion and nonlinearities the pulse shape is taking a broader shape with distance.

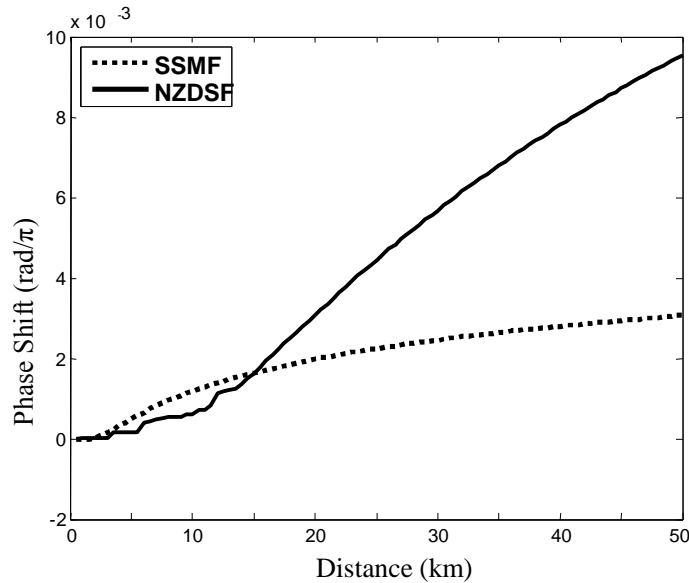## 4.2.2 Relation of Phase Fluctuation with Transmission Distance

Fig. 4.3: Phase shift versus distance for single fiber transmission

Fig 4.3 shows the IXPM induced phase fluctuation as a function of transmission distance for SSMF and NZDSF. The simulation is done for 50km propagation and at 40% duty cycle with a peak power of 1mW. The minimum pulse width (FWHM) is taken as 10ps and the pulses have a difference in time domain of 25ps. We can see that phase fluctuation increases linearly with the transmission distance from Fig. 4.3. The reason for higher phase fluctuations in NZDSF transmission is the smaller effective area of NZDSF .The effective core area of NZDSF is less ($50\mu m^2$) compared to SSMF ($80\mu m^2$). The non-linear effects that occur in optical fiber are proportional to power density and power density is inversely proportional to the effective area of the fiber. Power density increases with decreasing the effective area, A_{eff}.

4.2.3 Effect of Duty Cycle in Uncompensated Fiber Transmission

We explore the relation of phase fluctuations versus duty cycle for 40 Gb/s system with a peak power of 1mW. The duty cycle is 40% here. The transmission distance considered for this simulation is 50km and the pulses have a difference in time domain

of 25ps. Fig.4.4 shows that the phase shift is increasing for both uncompensated fiber transmission with larger duty cycle. The phase shift is highest when duty cycle is nearly 100%. It indicates the rapid increase of pulse to pulse interaction in the region $0 < d \leq 1$. It is evident from Fig.4.4 that SSMF shows lower phase variation compared to NZDSF.
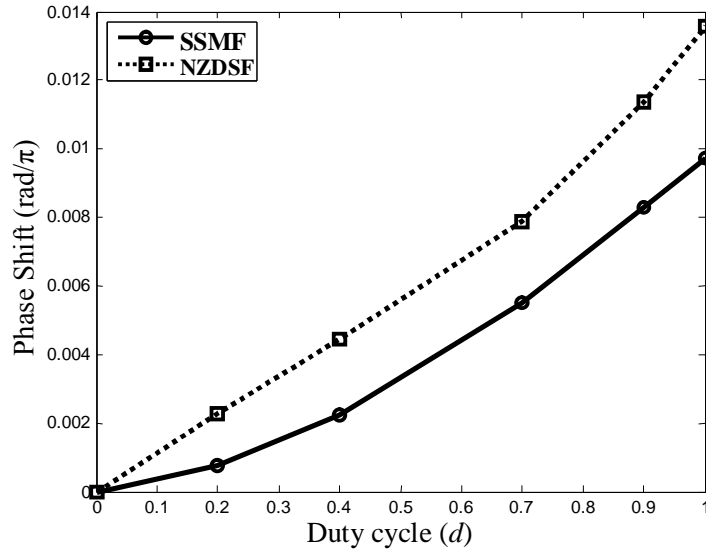

Fig. 4.4: Maximum phase fluctuation versus duty cycle for single fiber transmission

4.2.4 Effect of Input Power on Phase Fluctuation

The change in phase shift with the variation of power is shown in Fig. 4.5. Here the input pulse is operated at 40 Gb/s and duty cycle is 40%. Eq. (3.12) shows that the phase shift is directly related with the pulse energy. The analytical result shows that phase shift increases rapidly with the increase of peak power. The nonlinear refractive index causes an induced phase shift that is proportional to the intensity of pulse. Besides, Fiber nonlinearities arise from the refractive index of glass being dependent on the optical power which is given by the equation,

$$n = n_0 + n_2 \frac{P}{A_{eff}} \tag{4.1}$$

P is the power of the light wave inside the fiber and A_{eff} is the effective area of fiber core over which power is distributed. The intensity dependence of refractive index of silica leads to a large number of nonlinear effects, such as, SPM, XPM and FWM. The nonlinear refractive index causes an induced phase shift that is proportional to the

intensity of pulse. We can see that SSMF yields lower phase fluctuation compared to NZDSF.
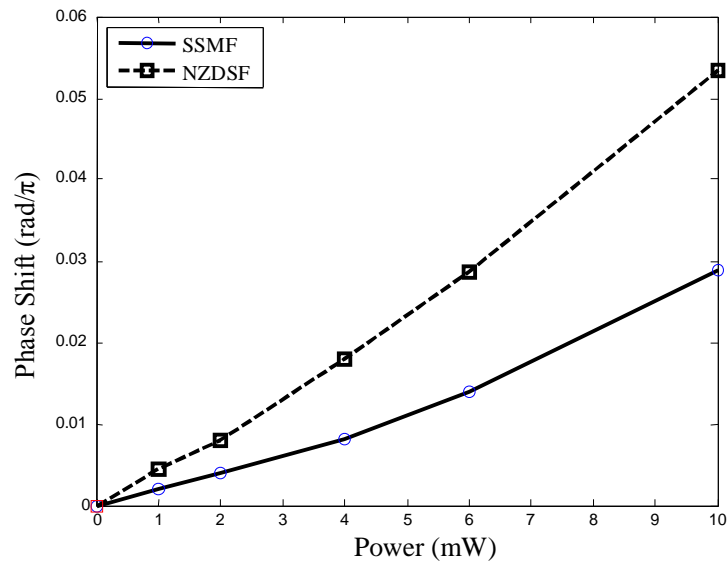

Fig .4.5: Phase shift versus initial peak power for 50km propagation

4.2.5 Drawbacks of Uncompensated Single Fiber Transmission

In fiber optic communication systems, information is transmitted over an optical fiber for more than 1000km. Several phenomena limit the transmission performance of long-haul optical transmission systems including fiber nonlinearities, dispersion, and noise [Govind, 2001]. The path length introduces a fundamental limit to single fiber communications. From Fig.4.2 we can see fiber chromatic dispersion and nonlinearity cause severe distortion in the pulse shape for only 100km propagation. It is very clear that for long-haul transmission the optical pulse can disperse, or spread, over a distance, which clearly can confuse the light detector at the far end of the fiber. A common method for overcoming this problem is dispersion management. For managing dispersion is to combine two or more types of single-mode fiber to produce the desired dispersion over the entire link span. The total dispersion can be set at virtually any value as the contributions from different components may have opposite signs (i.e. either positive or negative) and hence they can partially, or completely, cancel each other. Management of fiber dispersion can achieve by choosing optimal dispersion map. The technique is known as dispersion mapping.

4.3 System Description of DM System

We model a single channel transmission system with periodic dispersion compensation. We do not consider fiber loss for simplicity. We theoretically analyze the pulse behavior along the transmission fiber. We assume a two step periodic dispersion map as shown in Fig.4.6 for DM transmission line. Transmission line with highly dispersive fibers like standard single mode fiber (SSMF) and Non-zero dispersion–shifted fiber (NZDSF) are considered and dispersion compensating fiber (DCF) is used to control the total residual dispersion. We consider a periodic dispersion model, Model (A) has a period span of $L_1 + L_2 = 50$km which is repeated 20 times to cover the total transmission of around 1000km. For Model (A) SSMF is followed by DCF in each period where the length of SSMF is $L_1 = 43$km and length of DCF is $L_2 = 7$km. Model parameters for SSMF are taken as dispersion 17ps/nm/km, effective core area 80μm^2 and nonlinear index coefficient 2.5×10^{-20} m^2/W, when these are -100ps/nm/km, 20μm^2 and 3.0×10^{-20} m^2/W for DCF
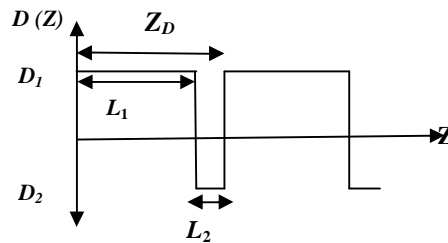

Fig. 4.6: Schematic diagram of a periodic two step dispersion map

.

In Model (B) we use NZDSF in place of SSMF. It has fiber parameters as following: dispersion parameter 4ps/nm/km, effective core area 50μm^2 and nonlinear index coefficient 1.5×10^{-20}m^2/W. Again for DCF these are -96ps/nm/km, 20μm^2 and 3.0 $\times 10^{-20}$ m^2/W for DCF. So we select the length of NZDSF $L_1 = 48$km and length of DCF $L_2 = 2$km. We assumed a bit rate of 40 Gb/s with peak power 1mW for each pulse with each of them having wavelength of 1.55μm. The pulses have pulse width 10ps and have a difference in time domain of 25ps. The length of DCF is chosen such that it satisfies the equation $L_1D_1 + L_2D_2 = 0$ for residual dispersion at the end of each period where D_1 and D_2 are dispersion parameters of SSMF and DCF.
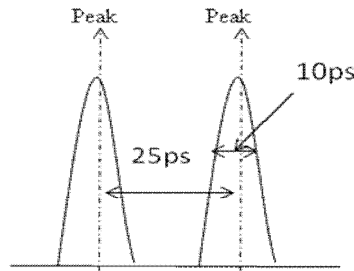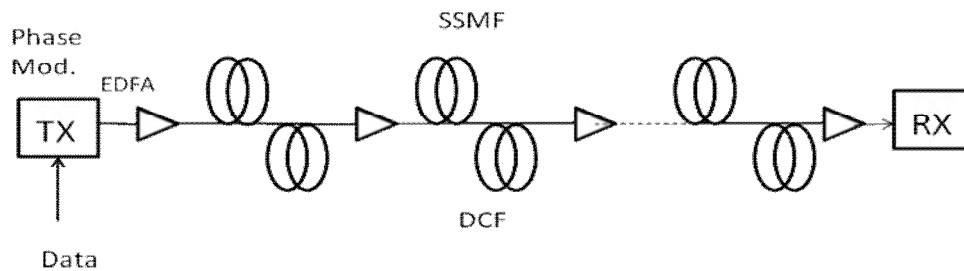
Fig. 4.7: Input pulse for both Model (A) and Model (B)
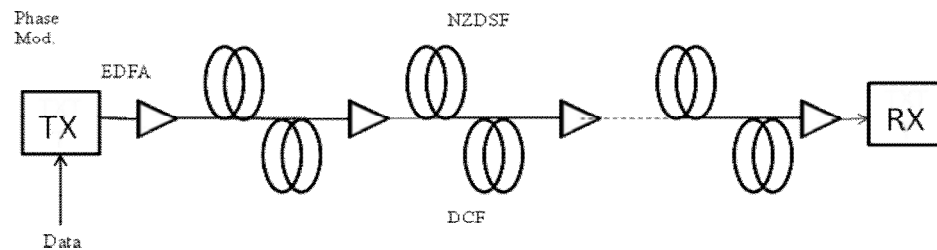
Model (A)

Model (B)

Figure 4.8: Transmission line models for Different DM system

4.3.1 Pulse Propagation in DM system

We numerically simulate the Gaussian pulse evolution in DM transmission system for the total transmission length of 1000 km. The numerical simulations have been carried out by directly solving Eq. (3.7) using split-step Fourier method taking into account the parameters mentioned above. We show pulse evolution along the periodic DM system for two DM map periods for Model (A) in Fig. 4.9. We observe stationary pulse propagation for a single pulse in a dispersion managed system.
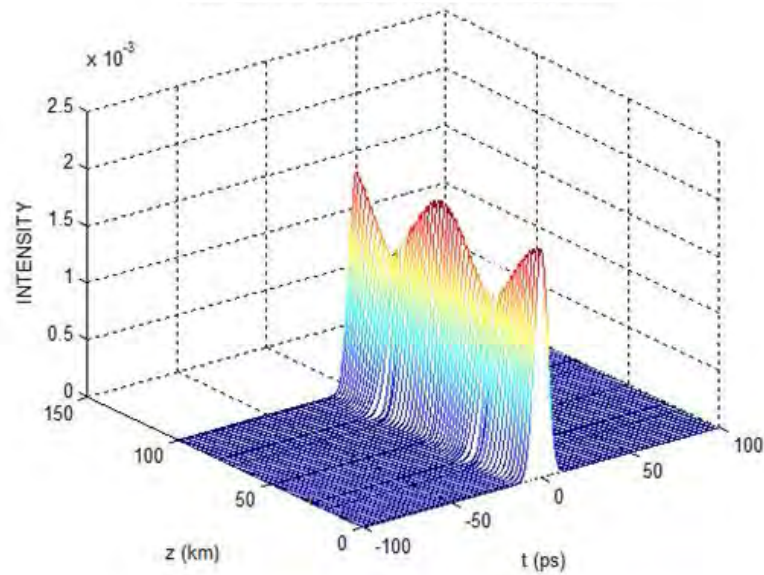
Fig 4.9: Single Pulse dynamics within the DM system (Model-A) with full numerical simulation for two DM map periods
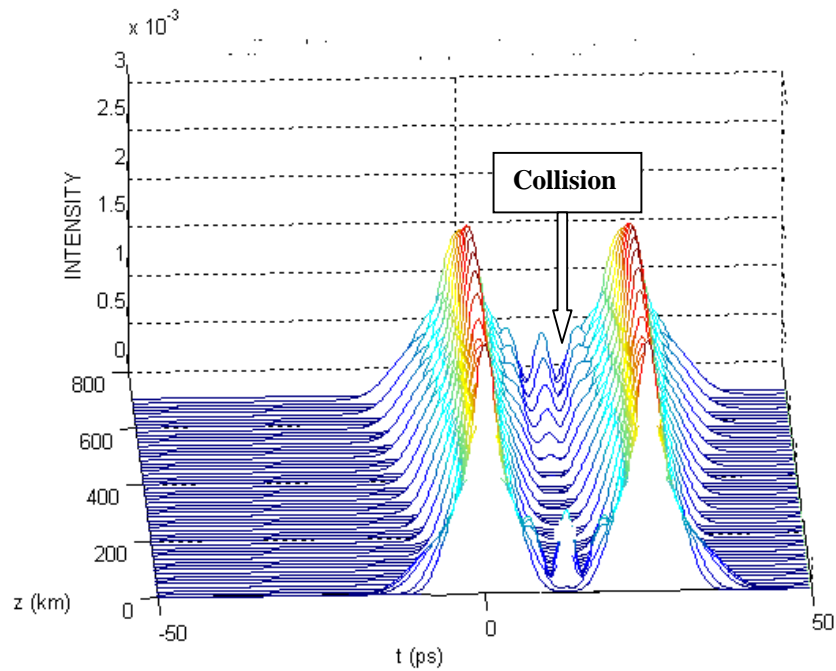

Fig 4.10: Plot of the pulse to pulse interaction due to IXPM in a DM system

To investigate the properties of two colliding DM pulses, we use simultaneously propagating pulses in the same channel separated by 25 ps. We simulate the Gaussian pulse evolution in single fiber transmission system for a transmission distance 700 km.

The pulse-to-pulse interaction is clearly observed in fig. 4.10. The figure shows that the two pulses keep their robustness up to $Z \approx 150$km before collision occurs along the propagation distance nearly at $Z=500$km.

4.3.2 Relation of Phase Fluctuation with Transmission Distance for Model (A) and Model (B)
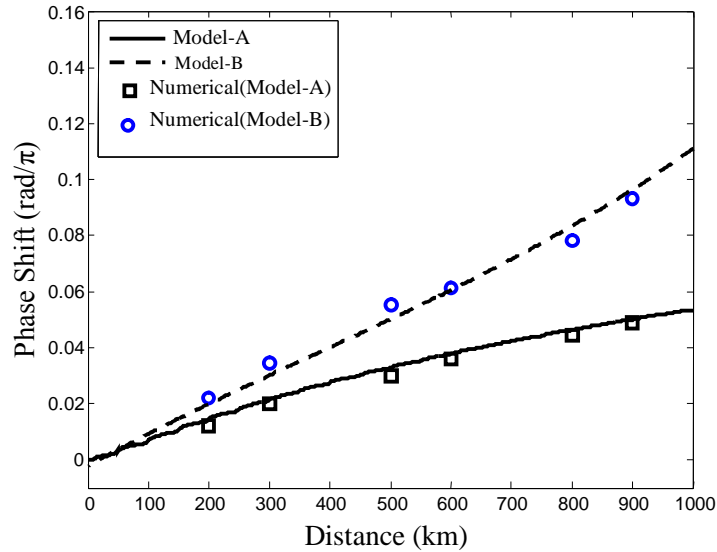

Fig.4.11: Phase shift versus transmission distance for DM Model (A) and Model (B)

Fig 4.11 shows maximum phase fluctuation is plotted against transmission distance for two types of DM Models both analytically and numerically for 1000km propagation. The simulation is done at 40% duty cycle with a power of 1mW. Phase fluctuation increases linearly with the transmission distance which is shown in Fig. 4.11. It can be said, path length introduces a fundamental limit to long-haul fiber communications. It is clear from the figure that the analytical estimation and numerical simulation results is satisfactory. We find that the Model (A) yields the lower phase shift compared to Model (B). The dispersion map strengths for Model (A) and Model (B) are 18.35 and 4.93 respectively. Lower DM map allow higher phase shift which is focused in sub-section 4.3.7. Again the reason for higher phase fluctuations of Model-(B) is the smaller effective area of NZDSF which is also focused in sub-section 4.2.2 .To realize a long haul transmission, a large effective area is essential to avoid nonlinear signal distortion. So Model (A) is more preferable to attain lower phase shift.

4.3.3 Effect of Power Variation on Phase Fluctuation

The change in phase shift for Model (A) with the variation of power is shown in Fig. 4.12. Here the input pulse is operated at 40 Gb/s and duty cycle is 40%. Eq. (3.12) shows that the phase shift is directly related with the pulse energy. The analytical result shows that phase shift increases rapidly with the increase of peak power which is also approved by the numerical result. Besides, in section 4.2.4 we have discussed that the nonlinear refractive index causes an induced phase shift that is proportional to the intensity of pulse. So we can say the magnitude of phase shift can be reduced by controlling the input power. On the other hand, minimizing power P is limited by the fact that during network design, there is a strong trade-off between non-linear effects and optical signal to noise ratio as decreasing P will decrease non-linear effects but also the signal to noise ratio (OSNR). The analytical prediction is supported by the numerical results.
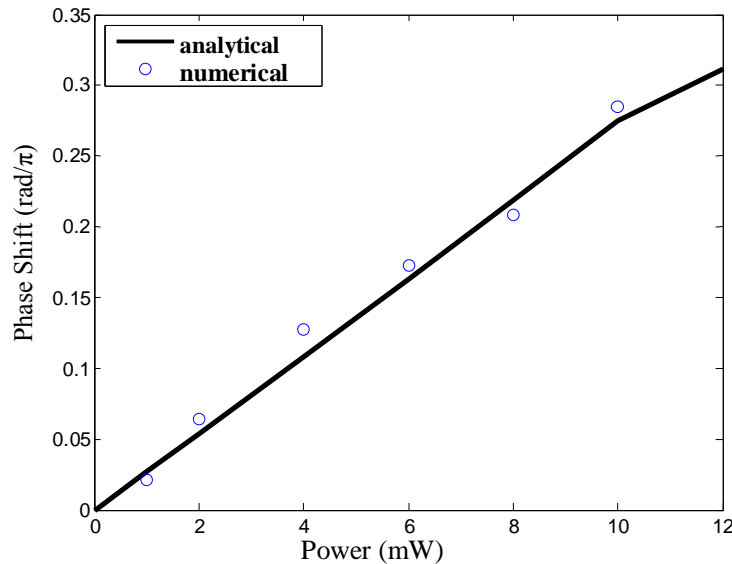

Fig. 4.12: Phase shift versus initial peak power for DM Model (A).

4.3.4 Effect of Duty Cycle

We explore the change of maximum phase shift as a function of duty cycle d for 40 Gb/s system with a peak power of 1mW. For illustration purpose the equation of two optical pulses can be written as:

$$U_1(0,t) = A_0 \exp\left(\frac{-t^2}{2T_0^2}\right)$$

(4.1)

$$U_2(0,t) = A_0 \exp\left(\frac{-(t-T)^2}{2T_0^2}\right)$$

Here T_0 is the half width (at is $1/e$ intensity point). In practice, it is customary to use the full width at half maximum in place of T_0. For Gaussian pulse, the two arte related a

$$\tau_F = 1.66T_0$$

So Eqn. (4.1) can be written as $U_1(0,t) = A_0 \exp\left(\frac{-1.386t^2}{2\tau_F^2}\right)$

Similarly for the second pulse $U_1(0,t) = A_0 \exp\left(\frac{-1.386(t-T)^2}{2\tau_F^2}\right)$

Here T the optical pulse separation which is kept constant which is 25ps and pulse width τ_F is varied. The action of intra-channel cross phase modulation can be described by $\frac{dU_1(t)}{dz} = j\gamma U_1(t)|U_2|^2$, with a phase shift of $\gamma|U_2|^2$, the instantaneous phase shift is

$$\frac{d\partial\phi_1(t)}{dz} = \gamma|U_2|^2 \quad \text{with a mean phase shift of}$$

$$\frac{d\Delta\phi_1}{dz} = \frac{\int \frac{d\partial\phi_1(t)}{dz}|U_1(t)|^2}{\int |U_1(t)|^2 dt}$$

Now the phase shift is can be expressed as

$$\frac{d\Delta\varphi_1}{dz} = \frac{\gamma p_0}{\sqrt{2\pi}} \frac{T}{\tau_F} \exp\left(\frac{-T^2}{2\tau_F^2}\right) \tag{4.2}$$

We can write Duty cycle $d = \frac{\tau_F}{T}$

Eq. (4.2) can be written as $\quad \frac{d\Delta\varphi_1}{dz} = \frac{\gamma p_0}{\sqrt{2\pi}} \frac{1}{d} \exp\left(\frac{-1}{2d^2}\right)$ (4.3)

We can see when from the equation (4.3) and also from Fig.4.13 when duty cycle ($d\ll 1$), no pulses overlap and the phase shift is less. As duty cycle d is increased, pulse broadens and the phase shift increases. Here the effect of IXPM depends on two factors: the level of pulse overlap and the intensity derivative in this context means the first derivative of pulse intensity. As interacting pulses are dispersed during propagation, their intensity derivatives are decreased while the pulse overlap region is increased. Therefore, when pulses strongly overlap each other, the intensity derivative of the pulses involved in the IXPM process is small due to the pulses being severely dispersed. On the other hand, the intensity derivative of the pulses is strong when the pulse overlap is

small (d<<1). Hence, the IXPM is strongest when pulses partially overlap ($d\approx 1$) due to the compromise between the intensity derivatives of the interacting pulses and the level of overlap. It is evident from Fig.4.13, after sufficient pulse broadening (d>>1), the effects of pulse-to-pulse interaction decrease rapidly. Fig. 4.13 shows two regions with small pulse-to-pulse interaction effect when FWHM pulse width is either much smaller or larger than pulse separation *T*.
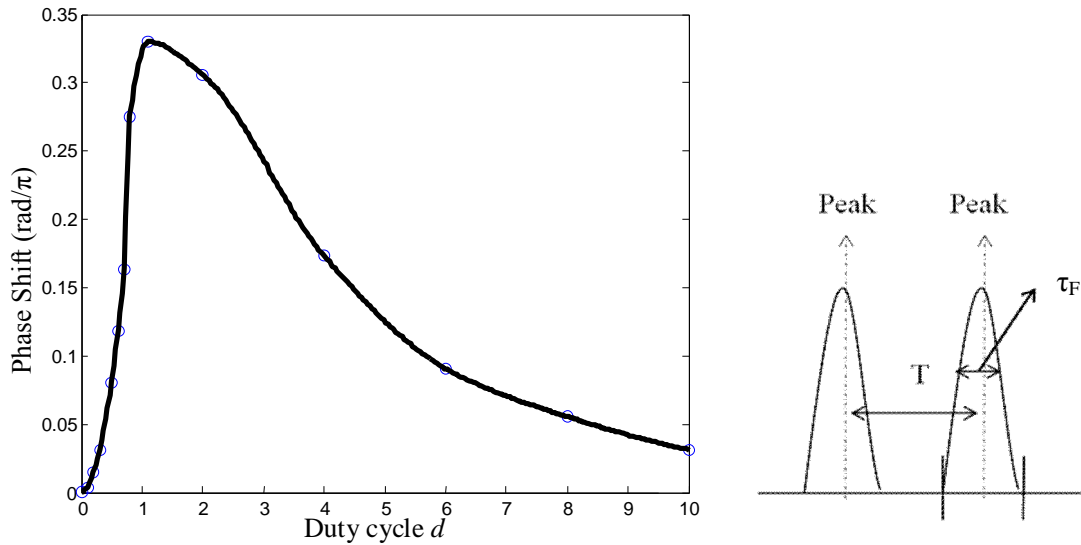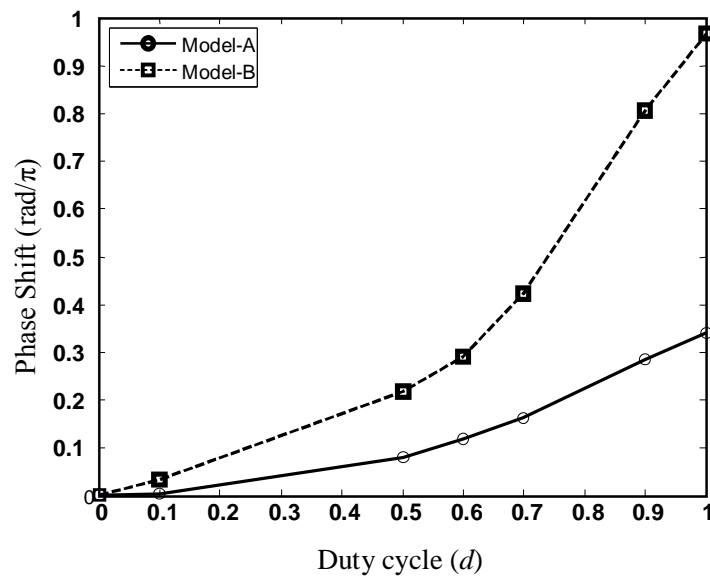

Fig 4.13: Phase shift as a function duty cycle

Fig. 4.14: Maximum phase shift versus duty cycle, *d* for Model (A) and Model (B)

Next we explore the change of maximum phase shift as a function of duty cycle *d* in Fig.4.14 for Model (A) and Model (B). It is evident that Model (A) shows lower phase

variation compared to Model (B). So to attain lower phase shift the optical pulse should be operated at lower duty cycle. On the other hand there is also a limit on the smaller value of duty cycle on the basis of its spectral bandwidth. Thus considering the spectral aspect of duty cycle, optimum value of duty cycle should be chosen so that phase fluctuations remain low.

4.3.5 Effect of Bit period on Phase Fluctuation

The effect of initial bit interval T on phase shift is plotted in Fig. 4.15. We vary T and plot the maximum phase shift for Model (A) with a peak power 1mW and 4mW at 40% duty cycle. Here the pulse width (FWHM) is kept constant which is 10ps. The results show that phase shift is sensitive to bit interval and the same model with greater power levels experiences higher IXPM effect for a certain range of bit interval. We can see the phase shift increases as the bit period decreases. We can approximately predict that maximum phase shift is inversely proportional to bit interval.
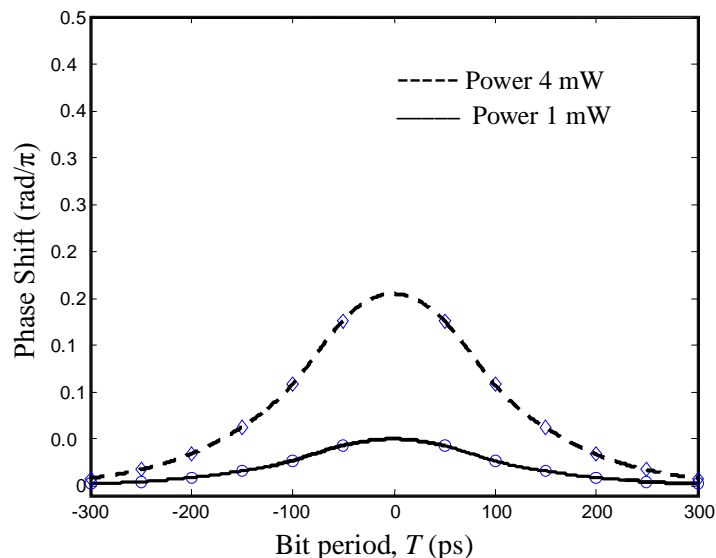
Fig. 4.15: Phase shift versus initial bit period *(T)* for Model (A) for 1000km propagation

4.3.6 Effect of Bit Rate (R_b)

Next we explore the relationship between phase fluctuations and transmission bit rate for Model (A) and Model (B) in Fig. 4.16. The system is operated at 50% duty cycle with a peak power of 2mW. The influence of IXPM is dominant at bit rate 40Gb/s and above. A continuous increase in phase shift is observed with increasing bit rate because pulse-to-

pulse interaction increases with higher bit rates. Besides if we increase bit rate, the power spectrum of the channel spreads and this increase the IXPM power transfer [28]. It is difficult for an optical receiver to differentiate one pulse from another if the power spectrum of the channel spreads. We can see that Model (A) shows lower phase variation compared to Model (B). Thus considering the spectral aspect, bit rate should be optimized for long haul transmission system.
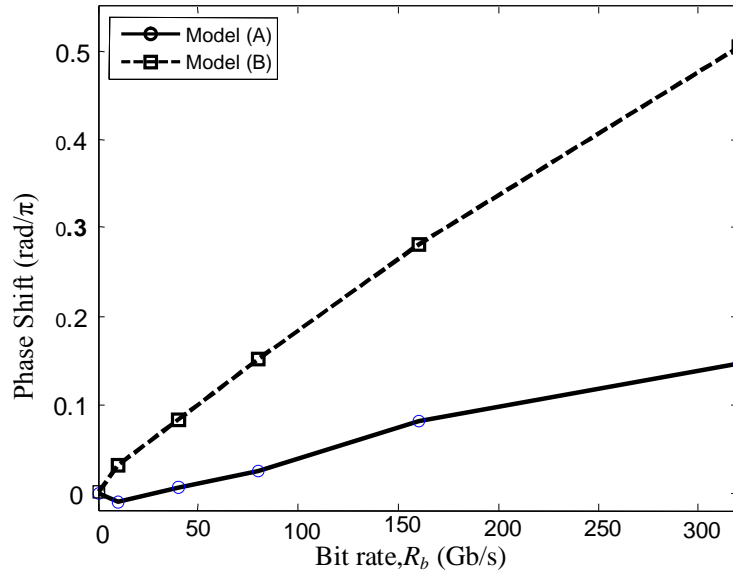

Fig.4.16: Phase shift versus bit rate R_b for both DM Model

4.3.7 Effect of Dispersion Map Strength (S)

The analytical expression of the dimensionless dispersion map strength S which indicates the degree of DM effects is given as [29], S=$(-b_1L_1+b_2L_2)/\tau_F^2$, where b_1 , L_1 ,b_2 ,L_2 are dispersion co-efficient and lengths of two fiber sections constituting the DM map period ($z_1 +z_2 = z_D$) and τ_F is the minimum pulse width (FWHM). The pulses have pulse width 10ps. We vary dispersion map strength S by changing DM map period ($z_1 +z_2 = z_d$) and keeping other variables constant. The dispersion map strength for 21.06km, 28.08km, 41km, 60.84km and 70.2km are 7.8, 10.5, 15.3, 22.68 and 26.1 respectively. Fig.4.17 is the plot of phase shift as a function of dispersion strength for 1000km. We can see the phase shift decreases with map strength. Weaker DM maps allow higher phase shift because the amount of nonlinear effects reduces with the increase of dispersion map strength. The physical reason is that in strongly dispersion compensated line, pulse width expands much more for a constant energy compared to a weaker one and the peak power

is suppressed locally, as a result the effect of SPM is diluted. Therefore fiber nonlinearity induced phase shift becomes smaller for stronger dispersion compensated line.
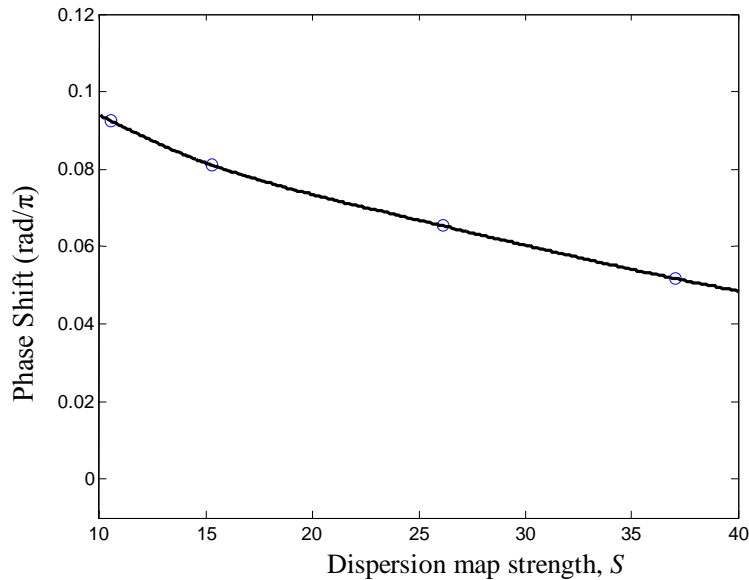

Fig.4.17. Phase shift versus Dispersion map strength with a peak power of 1mw

4.4 Conclusion

Intra-channel cross phase modulation is not significant for 10 Gb/s line and can be neglected. So, we are more interested in 40 Gb/s line pulse propagation. For this reason our analyses are done for 40 Gb/s system. Numerical analysis gives almost the same results as analytical in some cases. Which means the assumptions and parametric calculations were not wrong.

From Fig. 4.2, we can see the propagation of two a pulse in a single fiber transmission for 100km. As a result of intra-channel dispersion, the pulse is distorted and broadened with only 100km propagation. The relation of IXPM induced phase fluctuation in an uncompensated single line transmission are shown in Fig. 4.3 to Fig.4.5 for SSMF and NZDSF system as a function of transmission distance; duty cycle and power. For both cases the phase shift increase with all these parameters. We can say SSMF can be used for single fiber communication to attain lower phase fluctuation. From Fig.4.2 we can see fiber dispersion and nonlinearity cause severe distortion in the pulse shape for only 100km propagation. It is very clear that for long-haul transmission the optical pulse can disperse and get distorted in uncompensated line. A common method for overcoming this distortion problem is the dispersion management system.

Next we model a single channel transmission system with periodic dispersion compensation. From Fig. 4.8 and 4.9; we can see the propagation of two pulses in a single channel transmission. We investigate the pulse to pulse interaction due to IXPM in a DM system. It is clear that two pulses keep their robustness up to $Z \approx 150$km before collision occurs along the propagation distance nearly at Z=600km. In Fig. 4.11 and Fig. 4.12, phase fluctuation is observed varying transmission distance and power respectively. It has been seen that the maximum phase-shift increases almost proportionally to the power and distance. The phase shift is almost linear to the change of power and transmission distance which is obtained both numerically and analytically.

It is evident from Figure 4.11, 4.14 and 4.16 that Model (A) yields better performance compared to Model (B). So, DM Model (A) is a good solution for long haul transmission for pulse. It has been found that the amount of phase shift increases with the increase of duty cycle, bit rate and input power. We can predict that transmission quality of optical transmission system can be improved if the launched optical power P is minimized and/or the effective area of the fiber A_{eff} is maximized. Minimizing P is limited by the fact that during network design, there is a strong trade-off between non-linear effects and optical signal to noise ratio (decreasing P will decrease non-linear effects but also the OSNR). On the other hand, phase fluctuation decreases with the increase of bit period and dispersion map strength which is focused in Fig. 4.15 and 4.17 respectively. It can be said that an optimum model can be designed if a 40 Gb/s RZ pulse is used by lowering input power, duty cycle and increasing dispersion map strength. Finally transmission bit rate should be optimized for long haul transmission system considering the spectral aspect.

CHAPTER 5
CONCLUSION

5.1 Summary

This thesis has been devoted to the investigation of phase fluctuations in dispersion-managed optical fiber transmission systems in order to obtain long-haul high capacity optical communication networks. In this study, we have explored the impact of fiber nonlinearity, mainly IXPM, and chromatic dispersion on single fiber transmission and we have mainly focused on the IXPM induced phase fluctuations in a single channel DM system. First analytical estimation for phase shift has been deduced using variational analysis. We have obtained several ordinary differential equations for various pulse parameters. These pulse parameters are amplitude (A), reciprocal of pulse width (p), linear chirp (C), central frequency (κ), central time position (T) and the phase of the pulse (θ). These ordinary differential equations have been solved by Runge-Kutta method to find out the phase fluctuations due to IXPM. Next the effects of various parameters such as input power, bit interval, duty cycle, dispersion map strength and bit-rate on phase shift have been studied. The amount of phase shift due to IXPM is also investigated for different DM transmission model system, changing different parameters. Finally, split step Fourier method (SSFM) is used for full numerical simulation in some cases and to check the validity of analytical simulation. The outcome of this thesis is the development of analytical model for phase fluctuations and the exploration of the parameters that could affect phase shift due to IXPM. Finally the optimum model will be investigated for designing ultra-high speed phase modulated transmission systems so that IXPM-induced phase fluctuations remain low.

Chapter 2 gives a brief description of fiber nonlinearities and impairments of optical fiber communication. The motivations for working with IXPM are focused here.

The fundamental equation for optical pulse propagation in a fiber has been introduced considering a Gaussian solution of NLS equation in chapter 3. Next

the methods used for analyzing the intra-channel phase shift are briefly given. Different ordinary differential equations for various pulse parameters are deduced using variational method, which is an analytic technique to observe the phase shift at different distance of an optical pulse. Then we used the numerical method, SSFM to check the results observed by the analytic technique. Both this techniques are described in this chapter for dispersion management system.

Chapter 4 provides the results of our experiment. First, we have discussed the specification of the different models used for our experiments. Then the analytic and numerical plots are given for these models with respect to different parameters. From the results obtained, it can be concluded that phase fluctuations due to fiber nonlinearity might be a major limiting factor in the way to realize long-haul high speed phase modulated transmission systems. It is clearly seen that the performance degradations are mainly due to the nonlinear effects that occur when there is overlap between dispersed pulses regardless of whether dispersion compensation is deployed. Non-linear effects are due to the fact that the optical properties of the medium (refractive index, loss, etc.) become dependent of the transmission length (distance between the transmitter and the receiver), the type of fiber, field intensity, the cross-sectional area of the fiber, wavelength and duty cycle. Basically, these effects become more intensive when the optical power or the transmission length increases or when the pulse to pulse spacing becomes narrower. As a consequence, intra-channel nonlinearities can impose significant limitations on high bit-rates (40 Gb/s and higher), Long Haul (LH) and Ultra-Long Haul (ULH) systems. However, these impairments could be mitigated by properly designing DM transmission systems along with consideration of other parameters. It has been found that the amount of phase shift increases with increasing input power, duty cycle and bit rate for both uncompensated and DM system. On the other hand, phase fluctuation decreases with the increase of dispersion map strength. It is evident that the DM Model (A) yields better performance compared to DM Model (B). We can predict that transmission quality of optical transmission system can be improved if a 40 Gb/s RZ pulse is used as input by lowering duty cycle and input power. The results show that the reduction of phase fluctuation is possible by appropriately choosing the dispersion management map strength. In some cases our results obtained by variational analysis are validated by numerical simulations. Finally, we can propose upgraded models for quasi-linear systems which will offer lower phase fluctuations.

5.2 Future Work

In this thesis we have investigated optical pulse propagation in dispersion managed system but we have not considered noise and residual dispersion. So this investigation needs further modification by considering amplifier and receiver noise .Again, we have only considered single fiber transmission and dispersion management system. Corresponding transmitter and receiver and other supporting devices should be designed accordingly with this kind of dispersion managed system which we did not study in this thesis. So there are a lot of investigations yet to be done in this area. We have taken 40Gb/s systems here. But the bit rate is increasing to 80 Gb/s or even 160Gb/s now days. With increasing bit rate, IXPM effect is going to be more dominant in transmission line and contributing error along with the other errors. So, the IXPM induced phase shift must be investigated for these high speed lines and also for different kinds of modulation formats (DPSK, DQPSK, QPSK etc.).

As we have seen mainly DM Model (A) gives the better result than DM Model (B). Different DM models combining different fibers (SSMF, DCF, NZDSF, and DSF) can also be investigated which can be useful for more errorless propagation of optical signals. The effect of Fiber Bragg gratings can also be explored for DM system instead of DCF. More works are yet to be done to decrease IXPM in optical communication   system. Besides, IFWM is remarkably found to be deleterious for DM transmission system since it causes amplitude fluctuations, generate ghost pulses and introduce phase noise [16, 17]. Our analytical model and numerical simulation do not include these effects which is required to attain more practical results in high bit-rate systems.

However, we believe that our simplified analysis will support to perceive the essential physics of IXPM induced phase fluctuations which may provide useful information for designing phase modulated DM transmission systems.

Appendix A

Variational Analysis

The derivation of variational equations for optical pulse parameters is presented here. The basic equation which describes the optical pulse propagation with perturbation in a fiber is given as

$$i\frac{\partial U}{\partial Z} - \frac{b(Z)}{2}\frac{\partial^2 U}{\partial T^2} + S(Z)|U|^2 U = R(Z,T) \cdot \tag{A.1}$$

The description of its symbols and derivation are presented in Chapter 3. We know that this equation is not integrable because of varying coefficients $S(Z)$ and $b(Z)$ and perturbation term R. That's why, we apply Lagrangian variational method to simplify the equation and find an approximate solution assuming a known function. The Lagrangian density for the basic equation of optical pulse propagation in fiber given by A.1 can be obtained as

$$\mathrm{L} = \frac{i}{2}\left(U_Z U^* - U_Z^* U\right) + \frac{b(Z)}{2}|U_T|^2 + \frac{S(Z)}{2}|U|^4 - \left(U^* R + U R^*\right). \tag{A.2}$$

Now we derive the dynamical equations of optical pulse propagation in fiber that we described in Chapter 2. We assume the following *ansatz* (*solution*)

$$U(Z,T) = A(Z)f(\tau)\exp(i\varphi),$$

with $\tau(Z,T) = p(Z)\{T - T_0(Z)\}$, and

$$\varphi(Z,T) = \frac{C(Z)}{2}\tau^2 - \frac{\kappa(Z)}{p(Z)}\tau + \theta(Z). \tag{A.3}$$

Using this *ansatz*, we deduce the Lagrangian function L by integrating the Lagrangian density as

$$L = \int_{-\infty}^{\infty} \mathrm{L}\, dT$$

$$= \int_{-\infty}^{\infty}\left\{\frac{i}{2}\left(U_Z U^* - U_Z^* U\right) + \frac{b(Z)}{2}|U_T|^2 + \frac{S(Z)}{2}|U|^4 - \left(U^* R + U R^*\right)\right\} dT$$

$$= -\frac{A^2}{p}\left\{ I_C\left(\frac{1}{2}\frac{dC}{dZ}+\frac{C}{p}\frac{dp}{dZ}\right)+I_L\left(\kappa\frac{dT_0}{dZ}+\frac{d\theta}{dZ}\right)\right\}+I_N\frac{S(Z)A^4}{2p}$$

$$+\frac{b(Z)}{2}pA^2\left(I_D+I_CC^2+I_L\frac{\kappa^2}{p^2}\right)+N, \tag{A.4}$$

where I_C, I_D, I_L, and I_N are real constants defined by

$$I_C=\int_{-\infty}^{\infty}\tau^2f^2d\tau, \quad I_D=\int_{-\infty}^{\infty}\left(\frac{df}{d\tau}\right)^2d\tau, \quad I_L=\int_{-\infty}^{\infty}f^2d\tau, \quad I_N=\int_{-\infty}^{\infty}f^4d\tau, \tag{A.5}$$

and N is the noise term defined by

$$N=-\int_{-\infty}^{\infty}\left(U^*R+UR^*\right)dT. \tag{A.6}$$

We find that Lagrangian L is a function of x and its derivative with respect to Z, where x is any one of the parameters defined in Eq (A.3). Utilizing the well-known *Euler-Lagrange* equation we find

$$\frac{\partial L}{\partial x}-\frac{d}{dZ}\left(\frac{\partial L}{\partial x_Z}\right)=0. \tag{A.7}$$

Applying Eq. (A.4) to the above *Euler-Lagrange* equation, we find:

I. When $x=A$,

$$\frac{\partial L}{\partial A}-\frac{d}{dZ}\left(\frac{\partial L}{\partial A_Z}\right)=0$$

gives

$$-\frac{2A}{p}\left\{ I_C\left(\frac{1}{2}\frac{dC}{dZ}+\frac{C}{p}\frac{dp}{dZ}\right)+I_L\left(\kappa\frac{dT_0}{dZ}+\frac{d\theta}{dZ}\right)\right\}+\frac{2I_NS(Z)A^3}{p}$$

$$+b(Z)Ap\left(I_D+I_CC^2+I_L\frac{\kappa^2}{p^2}\right)+N_A=0,$$

$$I_C\left(\frac{C}{p}\frac{dp}{dZ}+\frac{1}{2}\frac{dC}{dZ}\right)+I_L\left(\kappa\frac{dT_0}{dZ}+\frac{d\theta}{dZ}\right)-I_NS(Z)A^2-\frac{b(Z)}{2}p^2\left(I_D+I_CC^2+I_L\frac{\kappa^2}{p^2}\right)=\frac{p}{2A}N_A, \tag{A.8}$$

where,

$$N_A=-\int_{-\infty}^{\infty}\left(\frac{\partial U^*}{\partial A}R+\frac{\partial U}{\partial A}R^*\right)dT. \tag{A.9}$$

II. When $x = p$,

$$\frac{\partial L}{\partial A} - \frac{d}{dZ}\left(\frac{\partial L}{\partial p_z}\right) = 0$$

gives

$$I_C\left(\frac{2C}{A}\frac{dA}{dZ} + \frac{3}{2}\frac{dC}{dZ}\right) + I_L\left(\kappa\frac{dT_0}{dZ} + \frac{d\theta}{dZ}\right) - I_N\frac{S(Z)A^2}{2}$$

$$+ \frac{b(Z)}{2}p^2\left(I_D + I_C C^2 - I_L\frac{\kappa^2}{p^2}\right) = -\frac{p^2}{A^2}N_p, \tag{A.10}$$

where,

$$N_p = -\int_{-\infty}^{\infty}\left(\frac{\partial U^*}{\partial p}R + \frac{\partial U}{\partial p}R^*\right)dT. \tag{A.11}$$

III. When $x = C$,

$$\frac{\partial L}{\partial C} - \frac{d}{dZ}\left(\frac{\partial L}{\partial C_z}\right) = 0$$

gives

$$I_C\left(-\frac{A}{p}\frac{dA}{dZ} + \frac{3}{2}\frac{A^2}{p^2}\frac{dp}{dZ} - b(Z)A^2 pC\right) = N_C, \tag{A.12}$$

where,

$$N_C = -\int_{-\infty}^{\infty}\left(\frac{\partial U^*}{\partial C}R + \frac{\partial U}{\partial C}R^*\right)dT. \tag{A.13}$$

IV. When $x = \kappa$,

$$\frac{\partial L}{\partial \kappa} - \frac{d}{dZ}\left(\frac{\partial L}{\partial \kappa_z}\right) = 0$$

Gives, $$-b(Z)\kappa + \frac{dT_0}{dZ} = \frac{p}{A^2 I_L}N_\kappa, \tag{A.14}$$

where,

$$N_\kappa = -\int_{-\infty}^{\infty}\left(\frac{\partial U^*}{\partial \kappa}R + \frac{\partial U}{\partial \kappa}R^*\right)dT. \tag{A.15}$$

V. When $x = T_0$,

$$\frac{\partial L}{\partial T_0} - \frac{d}{dZ}\left(\frac{\partial L}{\partial T_{0z}}\right) = 0$$

gives

$$\kappa\left(\frac{2}{A}\frac{dA}{dZ}-\frac{1}{p}\frac{dp}{dZ}\right)+\frac{d\kappa}{dZ}=-\frac{p}{I_LA^2}N_{T_0},$$ (A.16)

where, $N_{T_0}=-\int_{-\infty}^{\infty}\left(\frac{\partial U^*}{\partial T_0}R+\frac{\partial U}{\partial T_0}R^*\right)dT.$ (A.17)

VI. When $x=\theta$,
$$\frac{\partial L}{\partial\theta}-\frac{d}{dZ}\left(\frac{\partial L}{\partial\dot\theta}\right)=0$$

gives

$$\frac{2}{A}\frac{dA}{dZ}-\frac{1}{p}\frac{dp}{dZ}=-\frac{p}{I_LA^2}N_\theta,$$ (A.18)

where,

$$N_\theta=-\int_{-\infty}^{\infty}\left(\frac{\partial U^*}{\partial\theta}R+\frac{\partial U}{\partial\theta}R^*\right)dT.$$ (A.19)

Solving the coupled equations (A.41), (A.43), (A.45), (A.47), (A.49), and (A.51), the dynamics of the six pulse parameters under the perturbation can be determined as follows:

$$\frac{dA}{dZ}=\frac{b(Z)}{2}Ap^2C+R_A,$$ (A.20)

$$\frac{dp}{dZ}=b(Z)p^3C+R_p,$$ (A.21)

$$\frac{dC}{dZ}=-b(Z)p^2\left(\frac{I_D}{I_C}+C^2\right)-\frac{I_N}{2I_C}S(Z)A^2+R_C,$$ (A.22)

$$\frac{d\kappa}{dZ}=R_\kappa,$$ (A.23)

$$\frac{dT_0}{dZ}=b(Z)\kappa+R_{T_0},$$ (A.24)

$$\frac{d\theta}{dZ}=-b(Z)\left(\frac{\kappa^2}{2}-\frac{I_D}{I_L}p^2\right)+\frac{5I_N}{4I_L}S(Z)A^2+R_\theta,$$ (A.25)

where,

$$R_A=\frac{p}{2A}\left(\frac{N_C}{I_C}-\frac{3N_\theta}{2I_L}\right),$$ (A.26)

$$R_p=\frac{p^2}{A^2}\left(\frac{N_C}{I_C}-\frac{N_\theta}{2I_L}\right),$$ (A.27)

$$R_C = \frac{p}{A}\left(\frac{CN_\theta}{AI_L} - \frac{N_A}{2I_C} - \frac{pN_p}{AI_C}\right),$$

(A.28)

$$R_\kappa = \frac{p}{A^2 I_L}\left(\kappa N_\theta - N_{T_0}\right),$$

(A.29)

$$R_{T_0} = \frac{pN_\kappa}{A^2 I_L},$$

(A.30)

$$R_\theta = -\frac{p}{2AI_L}\left(\frac{2CN_C}{A} + \frac{2\kappa N_\kappa}{A} - \frac{3N_A}{2} - \frac{pN_p}{A}\right).$$

(A.31)

Assuming the Gaussian trial function, i.e., $f(\tau) = \exp\left(-\tau^2/2\right)$, the real constant I_C, I_D, I_L, and I_N are calculated as

$$I_C = \frac{\sqrt{\pi}}{2}, \quad I_D = \frac{\sqrt{\pi}}{2}, \quad I_L = \sqrt{\pi}, \quad I_N = \sqrt{\frac{\pi}{2}}.$$

(A.32)

Applying the above real constants the Eqs. (A.20) - (A.25) can be deduced as

$$\frac{dA}{dZ} = \frac{b(Z)}{2} A p^2 C + R_A,$$

(A.33)

$$\frac{dp}{dZ} = b(Z) p^3 C + R_p,$$

(A.34)

$$\frac{dC}{dZ} = -b(Z) p^2 \left(1 + C^2\right) - \frac{S(Z)}{\sqrt{2}} A^2 + R_C,$$

(A.35)

$$\frac{d\kappa}{dZ} = R_\kappa,$$

(A.36)

$$\frac{dT_0}{dZ} = b(Z)\kappa + R_{T_0},$$

(A.37)

$$\frac{d\theta}{dZ} = -\frac{b(Z)}{2}\left(\kappa^2 - p^2\right) + \frac{5S(Z)}{4\sqrt{2}} A^2 + R_\theta,$$

(A.38)

where,

$$R_A = \frac{1}{2\sqrt{\pi}}\int_{-\infty}^{\infty} \text{Im}\left[R e^{-i\varphi}\right]\left(3 - 2\tau^2\right)\exp\left(-\frac{\tau^2}{2}\right)d\tau,$$

(A.39)

$$R_p = \frac{p}{\sqrt{\pi}A}\int_{-\infty}^{\infty} \text{Im}\left[R e^{-i\varphi}\right]\left(1 - 2\tau^2\right)\exp\left(-\frac{\tau^2}{2}\right)d\tau,$$

(A.40)

$$R_C = \frac{2}{\sqrt{\pi}A}\int_{-\infty}^{\infty}\left\{\text{Re}\left[Re^{-i\varphi}\right] - C\,\text{Im}\left[Re^{-i\varphi}\right]\right\}\left(1-2\tau^2\right)\exp\left(-\frac{\tau^2}{2}\right)d\tau,$$ (A.41)

$$R_\kappa = \frac{2p}{\sqrt{\pi}A}\int_{-\infty}^{\infty}\left\{\text{Re}\left[Re^{-i\varphi}\right] - C\,\text{Im}\left[Re^{-i\varphi}\right]\right\}\tau\exp\left(-\frac{\tau^2}{2}\right)d\tau,$$ (A.42)

$$R_{T_0} = \frac{2}{\sqrt{\pi}Ap}\int_{-\infty}^{\infty}\text{Im}\left[Re^{-i\varphi}\right]\tau\exp\left(-\frac{\tau^2}{2}\right)d\tau,$$ (A.43)

$$R_\theta = -\frac{1}{2\sqrt{\pi}Ap}\int_{-\infty}^{\infty}\left\{p\,\text{Re}\left[Re^{-i\varphi}\right]\left(3-2\tau^2\right)+4\kappa\,\text{Im}\left[Re^{-i\varphi}\right]\tau\right\}\exp\left(-\frac{\tau^2}{2}\right)d\tau.$$ (A.44)

Here, $\text{Re}\left[Re^{-i\varphi}\right]$ and $\text{Im}\left[Re^{-i\varphi}\right]$ represent the real and imaginary parts of $Re^{-i\varphi}$, respectively. Now we develop the dynamical equations for single channel system with periodic dispersion management in order to estimate the phase fluctuations caused by IXPM. Assuming IXPM as the sole perturbation, R_j is can be defined as

$$R_j = -2S(Z)\left|U_{3-j}\right|^2 U_j = -2S(Z)A_{3-j}^2 A_j\exp\left(-\tau_{3-j}^2\right)\exp\left(-\frac{\tau_j^2}{2}\right)\exp\left(i\phi_j\right)$$ (A.45)

The dynamical equations with perturbation developed in Eq. (A.33-A.38) can be written for two pulses ($j = 1, 2$) as

$$\frac{dp_j}{dZ} = b(Z)p_j^3 C_j + R_{p_j},$$ (A.46)

$$\frac{dC_j}{dZ} = -b(Z)p_j^2\left(1+C_j^2\right) - \frac{S(Z)}{\sqrt{2}}A_j^2 + R_{C_j}$$ (A.47)

$$\frac{d\kappa_j}{dZ} = R_{\kappa_j},$$ (A.48)

$$\frac{dT_j}{dZ} = b(Z)\kappa_j + R_{T_j},$$ (A.49)

$$\frac{d\theta_j}{dZ} = -\frac{b(Z)}{2}\left(\kappa_j^2 - p_j^2\right) + \frac{5S(Z)}{4\sqrt{2}}A_j^2 + R_{\theta_j},$$ (A.50)

where

$$R_{p_j} = \frac{p_j}{\sqrt{\pi}A_j}\int_{-\infty}^{\infty}\text{Im}\left[R_j e^{-i\varphi_j}\right]\left(1-2\tau_j^2\right)\exp\left(-\frac{\tau_j^2}{2}\right)d\tau,$$ (A.51)

$$R_{C_j} = \frac{2}{\sqrt{\pi}A_j}\int_{-\infty}^{\infty}\left\{\text{Re}\left[R_j e^{-i\varphi_j}\right] - C_j\,\text{Im}\left[R_j e^{-i\varphi_j}\right]\right\}\left(1-2\tau_j^2\right)\exp\left(-\frac{\tau_j^2}{2}\right)d\tau,$$ (A.52)

$$R_{\kappa_j} = \frac{2p_j}{\sqrt{\pi}A_j}\int_{-\infty}^{\infty}\left\{\mathrm{Re}\left[R_j e^{-i\varphi_j}\right] - C_j\,\mathrm{Im}\left[R_j e^{-i\varphi_j}\right]\right\}\tau_j \exp\left(-\frac{\tau_j^2}{2}\right)d\tau,$$ (A.53)

$$R_{T_j} = \frac{2}{\sqrt{\pi}A_j p_j}\int_{-\infty}^{\infty}\mathrm{Im}\left[R_j e^{-i\varphi_j}\right]\tau_j \exp\left(-\frac{\tau_j^2}{2}\right)d\tau,$$ (A.54)

$$R_{\theta_j} = -\frac{1}{2\sqrt{\pi}A_j p_j}\int_{-\infty}^{\infty}\left\{p_j\,\mathrm{Re}\left[R_j e^{-i\varphi_j}\right]\left(3 - 2\tau_j^2\right) + 4\kappa_j\,\mathrm{Im}\left[R_j e^{-i\varphi_j}\right]\tau_j\right\}\exp\left(-\frac{\tau_j^2}{2}\right)d\tau.$$ (A.55)

Here $\mathrm{Re}\left[R_j e^{-i\varphi_j}\right]$ and $\mathrm{Im}\left[R_j e^{-i\varphi_j}\right]$ represent the real and imaginary parts of $R_j e^{-i\varphi_j}$, respectively, and can given as

$$\mathrm{Re}\left[R_j e^{-i\varphi_j}\right] = -2S(Z)A_{3-j}^2 A_j \exp\left(-\tau_{3-j}^2\right)\exp\left(-\frac{\tau_j^2}{2}\right)$$

$$\mathrm{Im}\left[R_j e^{-i\varphi_j}\right] = 0.$$

Now applying $E_j = \int_{\infty}^{\infty}\left|U_j\right|^2 dT = \sqrt{\pi}\,A_j^2/p_j$ which represents constant pulse energy of U_j, Eqs. (A.51) – (A.55) can be deduced as

$$R_{p_j} = 0,$$

$$
\begin{aligned}
R_{C_j} &= -\frac{4}{\sqrt{\pi}A_j}S(Z)\int_{-\infty}^{\infty}A_{3-j}^2 A_j \exp\left(-\tau_{3-j}^2\right)\exp\left(-\frac{\tau_j^2}{2}\right)\left(1 - 2\tau_j^2\right)\exp\left(-\frac{\tau_j^2}{2}\right)d\tau,\\
&= -\frac{4}{\pi}S(Z)E_{3-j}p_j p_{3-j}\int_{-\infty}^{\infty}\left\{1 - 2p_1^2\left(T - T_1\right)^2\right\}\exp\left\{-p_1^2\left(T - T_1\right)^2 - p_2^2\left(T - T_2\right)^2\right\}dT,\\
&= \frac{4}{\sqrt{\pi}}S(Z)E_{3-j}p_j p_{3-j}^3\,\frac{\left\{-p_1^2 - p_2^2 + 2p_1^2 p_2^2\left(T_1 - T_2\right)^2\right\}}{\left(p_1^2 + p_1^2\right)^{5/2}}\exp\left\{-\frac{p_1^2 p_2^2\left(T_1 - T_2\right)^2}{p_1^2 + p_2^2}\right\},\\
&= -4S(Z)\frac{E_{3-j}}{\sqrt{\pi}}\frac{p_j p_{3-j}^3}{P^5}\left\{P^2 - 2\left(\Delta\tau\right)^2\right\}F,
\end{aligned}
$$

$$
\begin{aligned}
R_{\kappa_j} &= -\frac{4}{\sqrt{\pi}A_j}S(Z)p_j\int_{-\infty}^{\infty}A_{3-j}^2 A_j \exp\left(-\tau_{3-j}^2\right)\exp\left(-\frac{\tau_j^2}{2}\right)\tau_j \exp\left(-\frac{\tau_j^2}{2}\right)d\tau,\\
&= -\frac{4}{\pi}S(Z)E_j p_1^2 p_2\int_{-\infty}^{\infty}p_1\left(T - T_2\right)\exp\left\{-p_1^2\left(T - T_1\right)^2 - p_2^2\left(T - T_2\right)^2\right\}dT,\\
&= \frac{4}{\sqrt{\pi}}S(Z)E_j p_1 p_2\,\frac{p_1^2 p_2^2\left(T_1 - T_2\right)\left(p_1^2 + p_2^2\right)}{\left(p_1^2 + p_1^2\right)^{5/2}}\exp\left\{-\frac{p_1^2 p_2^2\left(T_1 - T_2\right)^2}{p_1^2 + p_2^2}\right\},
\end{aligned}
$$

$$= (-1)^{3-j} 4 S(Z) \frac{E_j}{\sqrt{\pi}} \frac{p_1^2 p_2^2}{P^3} \Delta \tau F,$$

$$R_{T_j} = 0,$$

$$R_{\theta_j} = -\frac{1}{2\sqrt{\pi} A_j p_j} S(Z) \int_{-\infty}^{\infty} p_j A_{3-j}^2 A_j \exp\left(-\tau_{3-j}^2\right) \exp\left(-\frac{\tau_j^2}{2}\right) \left(3 - 2\tau_j^2\right) \exp\left(-\frac{\tau_j^2}{2}\right) d\tau.$$

$$= \frac{1}{\pi} S(Z) E_{3-j} p_2 \int_{-\infty}^{\infty} \left\{ 3 - 2 p_1^2 \left(T - T_1\right)^2 \right\} \exp\left\{ -p_1^2 \left(T - T_1\right)^2 - p_2^2 \left(T - T_2\right)^2 \right\} dT,$$

$$= \frac{1}{\sqrt{\pi}} S(Z) E_{3-j} p_1 p_2 \frac{\left[2\left(p_1^4 + 2 p_1^2 p_2^2 + p_2^4\right) + p_2^2 \left\{ p_1^2 + p_2^2 - 2 p_1^2 p_2^2 \left(T_1 - T_2\right)^2 \right\}\right]}{\left(p_1^2 + p_1^2\right)^{5/2}} \exp\left\{ -\frac{p_1^2 p_2^2 \left(T_1 - T_2\right)^2}{p_1^2 + p_2^2} \right\},$$

$$= S(Z) \frac{E_{3-j}}{\sqrt{\pi}} p_1 p_2 \frac{\left[2 P^4 + p_{3-j}^2 \left\{ P^2 - 2\left(\Delta \tau\right)^2 \right\}\right]}{P^5} \exp\left\{ -\left(\frac{\Delta \tau}{P}\right)^2 \right\},$$

$$= S(Z) \frac{E_{3-j}}{\sqrt{\pi}} \frac{p_1 p_2}{P^5} \left\{ P^2 \left(2 P^2 + p_{3-j}^2\right) - 2 p_{3-j}^2 \left(\Delta \tau\right)^2 \right\} F,$$

where $\Delta \tau = p_1 p_2 \left(T_1 - T_2\right)$, $P = \sqrt{p_1^2 + p_2^2}$, and $F = \exp\left\{ -\left(\Delta \tau / P\right)^2 \right\}$. Taking the above Eqs. are transformed into

$$\frac{dp_j}{dZ} = b(Z) p_j^3 C_j, \tag{A.56}$$

$$\frac{dC_j}{dZ} = -b(Z) p_j^2 \left(1 + C_j^2\right) - \frac{S(Z)}{\sqrt{2}} A_j^2 - 4 S(Z) \frac{E_{3-j}}{\sqrt{\pi}} \frac{p_j p_{3-j}^3}{P^5} \left\{ P^2 - 2\left(\Delta \tau\right)^2 \right\} F, \tag{A.57}$$

$$\frac{d\kappa_j}{dZ} = (-1)^{3-j} 4 S(Z) \frac{E_j}{\sqrt{\pi}} \frac{p_1^2 p_2^2}{P^3} \Delta \tau F, \tag{A.58}$$

$$\frac{dT_j}{dZ} = b(Z) \kappa_j, \tag{A.59}$$

$$\frac{d\theta_j}{dZ} = -\frac{b(Z)}{2} \left(\kappa_j^2 - p_j^2\right) + \frac{5 S(Z)}{4\sqrt{2}} A_j^2 + S(Z) \frac{E_{3-j}}{\sqrt{\pi}} \frac{p_1 p_2}{P^5} \left\{ P^2 \left(2 P^2 + p_{3-j}^2\right) - 2 p_{3-j}^2 \left(\Delta \tau\right)^2 \right\} F.$$

The frequency separation ($\Delta\kappa(Z)$) and pulse spacing ($\Delta T(Z)$) can be determined as

$$\Delta\kappa(Z) = \kappa_1(Z) - \kappa_2(Z), \tag{A.60}$$

$$\Delta T(Z) = T_1(Z) - T_2(Z). \tag{A.61}$$

Considering Eq. (A.60), Eq. (A.61) can be written in differential equation as

$$\frac{d(\Delta T)}{dZ} = b(Z)\Delta\kappa.$$

(A.62)

Using Eq. (B.60) and Eq. (B.61), $\Delta\tau = p_1 p_2 (T_1 - T_2)$ can be deduced in differential equation as

$$\frac{d(\Delta\tau)}{dZ} = b(Z)\left\{\left(p_1^2 C_1 + p_2^2 C_2\right)\Delta\tau + p_1 p_2 \Delta\kappa\right\}.$$

(A.63)

And using Eq. (B.65), Eq. (B.68) can be written in differential equation as

$$\frac{d(\Delta\kappa)}{dZ} = 4S(Z)\frac{E_1 + E_2}{\sqrt{\pi}}\frac{p_1^2 p_2^2 \Delta\tau}{P^3}F.$$

(A.64)

BIBLIOGRAPHY

[1]   A. H. Gnauck and P. J. Winzer, "Optical phase-shift-keyed transmission," *IEEE J. Lightwave Technol.,* vol. 23, no. 1, pp. 115-130, 2005.

[2]   C. Xu, X. Liu, L. F. Mollenauer, and X. Wei, "Comparison of return to-zero differential phase-shift keying and on-off keying in long-haul dispersion managed transmission," *IEEE photon. Technol. Lett.*, vol. 15, no. 4, pp. 617-619, 2003.

[3]   C. Malouin, J. Bennike, and T. J. Schmidt, "Differential phase-shift keying receiver design applied to strong optical filtering," *IEEE/OSA J. Lightwave Technol.*, vol. 25, no. 11, pp. 3536-3542, 2007.

[4]   P. J. Winzer and R. -J. Essiambre, "Advanced modulation formats for high capacity optical transport networks," *IEEE/OSA J. Lightwave Technol.*, vol. 24, no. 12, pp. 4711-4728, December, 2006

[5]   C. Xu, X. Liu, and X. Wei, "Differential phase-shift keying for high spectral efficiency optical transmission," *IEEE J. Select. Topics Quantum Electron.*, vol. 10, no. 2, pp. 281- 293, 2004

[6]   W. A. Atia and R. S. Bondurant, "Demonstration of return-to-zero signaling in both OOK and DPSK formats to improve receiver sensitivity in an optically preamplified   receiver," *Proc. LEOS 12th Annual Meeting*, vol. 1, pp. 226-227, 1999.

[7]   M. Daikoku, N. Yoshikane, and I. Morita, "Performance comparison of modulation formats for 40 Gbit/s DWDM transmission systems," *Proc. OFC/NFOEC 2005,* paperOFN2, CA, USA, 2005.

[8]   D. -S. Ly-Gagnon, K. Katoh, and K. Kikuchi, "Unrepeatered optical transmission of 20 Gbit/s quadrature phase-shift keying signals over 210 km using homodyne phase-diversity receiver and digital signal processing," *Elec. Lett.,* vol. 41, no. 4, pp. 206-207, 2005.

[9]   K. -P. Ho, "Performance degradation of phase-modulated systems due to nonlinear phas noise," *IEEE Photon. Technol. Lett.*, vol. 15, no. 9, pp. 1213-1215, 2003.

[10]   F. Zhang, "XPM statistics in 100% precompensated WDM transmission for OOK and DPSK formats," *IEEE photon. Technol. Lett.*, vol.21, no. 22, pp. 1707-1709, Nov.2009

[11]   M. Faisal, A. Maruta "Cross-phase modulation induced phase fluctuations in optical RZ pulse propagating in dispersion compensated WDM transmission system," *Opt. Comm.* , vol. 283, pp. 1899-1904, 2010.

[12]   A. Maruta, M. Faisal and T. Nakamura, "Influence of amplifier noise and cross-

phase modulation on phase in optical RZ pulse," *IEICE Technical Report*, pp. 85-89, OCS2008-121, 2009

[13]   R. -J. Essiambre, B. Mikkelsen, and G. Raybon, "Intra-channel cross-phase modulation and four-wave mixing in high-speed TDM systems", *IEEE Electron. Lett.*, Vol. 35, No. 18, Sep. 1999, pp. 1576-1578.

[14]   F. Zhang, C. -A. Bunge, and K. Petermann, "Analysis of nonlinear phase noise in single- channel return-to-zero differential phase-shift keying transmission systems," *Opt. Lett.,* vol. 31, no. 8, pp. 1038-1040, 2006 .

[15]   H. Kim, and A. H. Gnauck, "Experimental Investigation of the Performance Limitation of DPSK Systems Due to Nonlinear Phase Noise*", IEEE Photon. Technol. Lett.,* Vol. 15, No. 2, pp. 320-322, Feb. 2003

[16]   X. Wei and X. Liu, "Analysis of intrachannel four-wave mixing in differential phase shift keying transmission with large dispersion", *Opt. Lett.,* Vol. 28. No. 23, pp. 2300-2302, Dec. 2003.

[17]   F. Zhang, C-A. Bunge and K. Petermann, "Analysis of nonlinear phase noise in single channel return-to-zero differential phase shift keying transmission systems," *Opt. Lett.* vol. 31, pp. 1038-1040, 2006

[18]   K.-P. Ho, "Phase-modulated optical communication systems", Springer, 2005

[19]   A. P. T. Lau, S. Rabbani, and J. M. Kahn, "On the Statistics of Intrachannel Four-Wave   Mixing in Phase-Modulated Optical Communication Systems," *J. Lightwave Technol.*,   vol. 26, 2128- 2135 , 2008.

[20]   X. Wei and X. Liu, "Analysis of intra-channel four wave mixing in DPSK transmission with large dispersion," *Opt. Lett.,* Vol. 28, Issue 23, pp. 2300-2302 , 2003.

[21]   A. Maruta, and S. Tomioka, "Intra-channel cross-phase modulation induced phase shift in optical RZ pulse propagating in dispersion managed line," *The 23rd Annual Meeting of the IEEE Photonics Society,* Denver, USA, pp. 209-210, November, 2010

[22]   D. J. Kaup, "Perturbation theory for solitons in optical fibers," *Phys. Rev.* A, vol. 42,   no. 9, pp. 5689-5694, 1990.

[23]   Y.Aoki, K. Tajima, and I. Mito, "input Power Limits of Single-Mode Optical Fibers   due to Stimulated Brillouin Scattering in Optical Communication Systems," *J. of Lightwave Technol.*, Vol. 6, No. 10, 1998, pp. 710-719.

[24]   A. Hasegawa and Y. Kodama, "Guiding-center solitons in optical fibers," *Opt. Lett.,* vol.15, no. 24, pp. 1443-1445, December, 1990.

[25]   D. Anderson, "Variational approach to nonlinear pulse propagation in optical fibers," *Phys. Rev.* A, vol. 27, no. 6, pp. 3135-3145, 1983.

[26]   J. H. B. Nijhof, W. Forysiak, and N. J. Doran, "The averaging method for finding exactly periodic dispersion-managed solitons," *IEEE J. Selected Topics Quantum Electron.,* vol. 6, no. 2, pp. 330-336, 2000.

[27]   P. Kylemark, "Nonlinear Fiber Optical Technologies for Transmission and amplification," Technical report - Department of Micro technology and Nano Science, Chalmers University of Technology, 2004.

[28]   Ibrahim A. Murdas, "Influence of Various XPM Impairment in WDM Systems," *European Journal of Scientific Research*, vol.65, no.1 pp. 102-108, 2011.

[29]   A. M. Niculae, W. Forysiak, A. J. Gloag, J. H. B. Nijhof, and N. J. Doran," Soliton collisions with wavelength-division multiplexed systems with strong dispersion management," *Opt. Lett*. Vol. 23, No. 17 , 1998